DEVELOPMENT OF EM DATA INVERSION ALGORITHM USING IIM & CRUSTAL DEFORMATION STUDIES IN ANTARCTICA USING GPS DATA

A DISSERTATION

submitted towards the partial fulfillment of the

requirements for the award of the degree of

INTEGRATED MASTERS IN TECHNOLOGY

in

GEOPHYSICAL TECHNOLOGY

Submitted by:

AARTI KUMARI DWIVEDI

DEPARTMENT OF EARTH SCIENCES

INDIAN INSTITUTE OF TECHNOLOGY, ROORKEE

ROORKEE - 247667, INDIA

May 2015

1. CERTIFICATE

It is certified that the Int. M. Tech. thesis titled "Development of Inversion Algorithm for 2D EM Data using IIM & Crustal Deformation of Antarctica Using GPS Data" has been done by Ms. Aarti Kumari Dwivedi (E. No. 11411001) under our supervision. This report has been submitted towards partial fulfillment of Integrated M. Tech. requirements.

Prof. M. Israil
Professor
Department of Earth Sciences
Indian Institute of Technology Roorkee
Roorkee - 247667, India

Prof. P. K. Gupta
Professor
Department of Earth Sciences
Indian Institute of Technology Roorkee
Roorkee - 247667, India

2. DECLARATION

I hereby declare that the work which is presented in this thesis titled "DEVELOPMENT OF EM DATA INVERSIONALGORITHM USING IIM & CRUSTAL DEFORMATIONSTUDIES IN ANTARCTICA USING GPS DATA" in partial fulfillment towards the Integrated M. Tech) requirements submitted to the Department of Earth Science, IIT Roorkee is an authentic record of my own work carried out during the period from July 2014 to May 2015 under the guidance of Prof. P. K. Gupta, and Prof. M. Israil, Department of Computer Science and Engineering, IIT Roorkee.

I also declare that I have adhered to all principles of academic honesty and integrity and have not misrepresented or falsified any idea/data/fact/source in my submission. I understand that any violation of the above will be cause for disciplinary action by the Institute and can also evoke penal action from the sources which have thus not been properly cited or from whom proper permission has not been taken when needed. The matter embodied in this thesis, to the best of my knowledge, has not been submitted for the award of any other degree elsewhere.

Aarti Kumari Dwivedi
E.No. 11411001
Indian Institute of Technology Roorkee
Roorkee - 247667, India

3. ACKNOWLEDGEMENT

It is a matter of great pleasure for me to present my dissertation titled " Development of Inversion Algorithm for 2D EM Data using IIM Crustal Deformation of Antarctica Using GPS Data" in the partial fulfillment of the requirement for the award of Integrated Masters of Technology in Geophysical Technology at Indian Institute of Technology Roorkee.

First I would like to thank my parents Dr. Vijay Kumar Dwivedi, and Dr. Manju Dwivedi for the unconditional support, love, and blessings, without which I would not have had the motivation to work through the dissertation.

I would like to express my heartfelt gratitude and respect to my supervisors Prof. P. K. Gupta, and Prof. M. Israil for introducing me the topic of this dissertation, which has cemented in me the desire to pursue research. I would like to wholeheartedly acknowledge the constant guidance they have provided, which manifested as constructive criticism, valuable suggestions, co-operation and keen interest, from the very beginning to the end. Working under their guidance has also helped me locate my flaws and become a better student in the process.

I sincerely express my gratitude to Dr. V. K. Gahalaut, for giving me a place on his team for 35th Indian Science Expedition to Antarctica. Without his support and guidance, this dissertation would not have been possible. I would also like to thank Shri Satish Chandrapuri, NGRI for guiding me during my work in Antarctica. I express my heartfelt thanks to Dr. Sanjay Prajapati, and Dr. Joshi Catherine for guiding me on processing of GPS data.

I sincerely acknowledge the contribution of Arun Singh, Ph.D. Scholar in the Department of Earth Sciences, IIT Roorkee for his help with programming during the dissertation.

I express my sincere thanks to the technical staff of Department of Earth Sciences, especially to Mr. V. K. Saini, Mr. S. K. Sharma, Mr. Nayar, Mr. Rakesh and Mrs.

Joseph, who have helped me in all possible ways during the official work.

Finally, I would like to thank all the teachers in Department of Earth Sciences, and all scientists who have broken barriers of human knowledge which has given me the courage and motivation for pursuing research.

Aarti Kumari Dwivedi
E.No. 11411001
Indian Institute of Technology Roorkee
Roorkee - 247667, India

4. ABSTRACT

This dissertation deals with the development of an inversion algorithm for 2D EM data using Immersed Interface Method. The implementation of forward modelling shows appropriate results and the inverse problem gives results in agreement with the established results.

Part 2 of the dissertation deals with the deformation at MAIT(Maitri), an Indian GPS site in Antarctica during the period January 2015 to February 2016. According to the study the plate motion at the site is 6mm/year North, and 2 mm/year East. This is in close agreement with previous studies.

Contents

1 CERTIFICATE i

2 DECLARATION ii

3 ACKNOWLEDGEMENT iii

4 ABSTRACT v

I Development of 2D EM Data Inversion Algorithm using IIM 2

5 INTRODUCTION TO ELECTROMAGNETIC THEORY 3

6 IMMERSED INTERFACE METHOD 6

7 FORWARD PROBLEM 10

8 INVERSE PROBLEM 14

9 RESULTS - IIM 16

9.1 Half-Space Model 16

9.2 Single Conductive Anomaly 18

9.3 Single Resistive Anomaly 20

9.4 One Conductive, One Resistive Anomaly 22

9.5 One Resistive, One Conductive Anomaly 24

II Crustal Deformation Studies in Antarctica using GPS

Data **26**

10 INTRODUCTION TO GPS **27**

11 INTRODUCTION TO ANTARCTICA **28**

11.1 MAITRI 28

12 TOOLS USED FOR PROCESSING **29**

13 ERROR SOURCES IN GPS **31**

14 VELOCITY ESTIMATE **39**

15 REFERENCES **57**

16 APPENDIX **60**

16.1 Subroutine for IIM 60

List of Figures

7.1 Points in FDM Stencil 10

9.1 Half-space 16
9.2 Half-space IIM 16
9.3 Half-space IIM 17
9.4 Single Conductive Anomaly 18
9.5 Single Conductive Heterogeneity IIM 18
9.6 Single Conductive Heterogeneity FDM 19
9.7 Single Resistive Anomaly 20
9.8 Single Resistive Heterogeneity IIM 20
9.9 Single Resistive Heterogeneity FDM 21
9.10 One Conductive, One Resistive Anomaly 22
9.11 One conductive anomaly, and one resistive anomaly IIM 22
9.12 One conductive anomaly, and one resistive anomaly FDM 23
9.13 One Resistive, One Conductive Anomaly 24
9.14 One resistive anomaly, and one conductive anomaly IIM 24
9.15 One resistive anomaly, and one conductive anomaly FDM 25

13.1 Sky plot at CAS1 33
13.2 Sky plot at DGAR 33
13.3 Sky plot at SYOG 34
13.4 Sky plot at HRAO 34
13.5 Sky plot at IISC 35
13.6 Sky plot at MAIT 35
13.7 Sky plot at MAW1 36
13.8 Sky plot at MCM4 36

13.9 Sky plot at PERT 37
13.10Sky plot at ROTH 37
13.11Sky plot at SEY1 38

14.1 Time series for KERG, January 2016 40
14.2 Time series for MAIT, January 2016 41
14.3 Time series for MAW1, January 2016 42
14.4 Time series for mcm41, January 2016 43
14.5 Time series for PERT, January 2016 44
14.6 Time series for ROTH, January 2016 45
14.7 Time series for SEY1, January 2016 46
14.8 Time series for SYOG, January 2016 47
14.9 Time series for KERG, Jan 2015, and Jan 2016, showing the movement of site 48
14.10Time series for MAIT, Jan 2015, and Jan 2016, showing the movement of site 49
14.11Time series for MAW1, Jan 2015, and Jan 2016, showing the movement of site 50
14.12Time series for mcm4, Jan 2015, and Jan 2016, showing the movement of site 51
14.13Time series for PERT, Jan 2015, and Jan 2016, showing the movement of site 52
14.14Time series for ROTH, Jan 2015, and Jan 2016, showing the movement of site 53
14.15Time series for SEY1, Jan 2015, and Jan 2016, showing the movement of site 54
14.16Time series for SYOG, Jan 2015, and Jan 2016, showing the movement of site 55
14.17Map of Antarctica with velocity estimates 56

List of Tables

9.1 Errors - Half Space 16
9.2 Errors - Single Conductive Anomaly 18
9.3 Errors - Single Resistive Anomaly 20
9.4 Errors - One conductive anomaly, and one resistive anomaly 22
9.5 Errors - One resistive anomaly, and one conductive anomaly 24

14.1 Velocity Estimates 39

Part I

Development of 2D EM Data Inversion Algorithm using IIM

5. INTRODUCTION TO ELECTROMAGNETIC THEORY

The geoelectromagnetic methods give information on the subsurface structure by giving information on the electrical properties of materials in the subsurface using electromagnetic field data. The observations are analysed as a combination of a primary, and secondary field, with the the primary field is caused by background sources. In the absence of any inhomogeneity, the secondary fields from secondary current, which were induced by primary current would follow a regular pattern. It is the perturbation in the total EM field(caused by a perturbed secondary field) that gives us an insight into the subsurface structure and processes.

We will formulate the forward model in this section.

A brief overview to electromagnetic theory is presented here. The laws governing EM fields are Biot-Savart's law governing magnetic field due to current, Coulomb law governing electric field due to charges, and law of non-existence of magnetic monopoles. Maxwell's equations summarize and integrate these laws in a mathematical form. In an inertial reference frame and for a linear, isotropic medium the Maxwell's equations are stated as:

$$\nabla \cdot \vec{E} = \frac{\rho}{\epsilon} \tag{5.1}$$

$$\nabla \cdot \vec{B} = 0 \tag{5.2}$$

$$\nabla \times \vec{E} = -\frac{\partial B}{\partial t} \tag{5.3}$$

$$\nabla \times \vec{B} = \mu_0 \vec{J} + \tag{5.4}$$

$$\mu_0 \epsilon \frac{\partial E}{\partial t} \tag{5.5}$$

with

$$\nabla = \frac{\partial}{\partial x}\hat{i} + \frac{\partial}{\partial y}\hat{j} + \frac{\partial}{\partial z}\hat{k} \tag{5.6}$$

The constitutive relations for Maxwell's equations are

$$\vec{J} = \sigma\vec{E}\vec{D} = \epsilon\vec{E}\vec{B} = \mu_0\vec{H} \tag{5.7}$$

It is acceptable to use μ_0 in place of μ due to the negligible difference between the two for most cases. The boundary conditions that are applicable to electromagnetic field in case of an interface between two materials are:

$$n \times (\vec{E_2} - \vec{E_1}) = 0 \tag{5.8}$$

$$n \times (\vec{H_2} - \vec{H_1}) = J_s \tag{5.9}$$

$$n \times (\vec{D_2} - \vec{D_1}) = \rho_s \tag{5.10}$$

$$n \times (\vec{B_2} - \vec{B_1}) = 0 \tag{5.11}$$

$$n \times (\vec{J_2} - \vec{J_1}) = 0 \tag{5.12}$$

where n is the unit vector normal to the interface, J_s is the current density on the surface, and ρ_s is the surface current density. For the case of Earth, given the depth of investigations normally used, and the property of subsurface materials, two assumptions are applicable to MT:

- In the period 10^{-5} to 10^5, displacement current is ignored since it is small in comparison to conductivity currents.
- The primary field is planar and propagates through the Earth vertically.
- Earth is a source-free, and passive medium.

This comes with the assumption of treating Earth as a linear, isotropic medium.

The time dependence is assumed to be of the form $e^{i\omega t}$, which leads to the following equations:

$$\nabla \cdot \vec{D} = 0 \tag{5.13}$$

$$\nabla \cdot \vec{B} = 0 \tag{5.14}$$

$$\nabla \times \vec{E} = -i\omega\mu_0\vec{H} \tag{5.15}$$

$$\nabla \times \vec{H} = \sigma\vec{E} \tag{5.16}$$

Some substitutions after Taking the curl of equation 3.12 and 3.13 lead us to the following equations,

$$\nabla \times \nabla \times \vec{E} = -i\omega\mu_0\sigma\vec{E} \tag{5.17}$$

$$\nabla \times (\rho\nabla \times \vec{H}) = -i\omega\mu_0\vec{H} \tag{5.18}$$

where ρ is the resistivity of the medium.

These equations are further reduced to the form

$$\nabla^2\vec{E} + k^2\vec{E} = 0 \tag{5.19}$$

$$\rho\nabla^2\vec{H} + \nabla\rho \times (\nabla \times \vec{H}) + k^2\vec{H} = 0 \tag{5.20}$$

where, k is the wave number, given by $k = -i\omega\mu_0\sigma$

The relationship between skin depth(in metres) and wave number is:

$$k = \frac{1+i}{\delta} \tag{5.21}$$

where $\delta = \sqrt{\frac{2}{\omega\mu\sigma}}$ is the skin depth.

6. IMMERSED INTERFACE METHOD

In this chapter we will attempt to discuss IIM for an elliptic equation of the form

$$(\beta u_x)_x + (\beta u_y)_y + k(x,y)u = f(x,y), (x,y) \in \Omega = \Omega^+ \cap \Omega^- \tag{6.1}$$

with boundary condition on $\partial\Omega$, where $\beta \geq \beta_m in \geq 0$ and σ and f are piecewise continuous but within the domain Ω they might be discontinuous across an interface. The problem is well-posed when there are two interface conditions, defined by

$$[u] = u^+ - u^- = w \tag{6.2}$$

$$[\beta u_n] = \beta^+ \frac{\partial u^+}{\partial n} - \beta^- \frac{\partial u^-}{\partial n} = v \tag{6.3}$$

where w and v are defined only along the interface.

Before proceeding, it is important to remember the importance of local coordinates in case of IIM. If θ is the angle between the X-axis and the normal from the interface in the direction of '+' side, then a point (x, y) will have to undergo transformation with respect to (X, Y), where (X, Y) is a point on the interface. The transformation is as follows:

$$\xi = (x - X)cos(\theta) + (y - Y)sin(\theta) \tag{6.4}$$

$$\eta = -(x - X)sin(\theta) + (y - Y)cos(\theta) \tag{6.5}$$

The quantity χ represents the curvature of the interface at (X, Y).
The local coordinates of (x_{i+i+k}, y_{j+j_k}) are (ξ_k, η_k). We will define regular and irregular points before proceeding to further description of IIM. A point is said to be *regular* if all the grid points in its stencil are on the same side of the interface. Similarly, a point is said to be *irregular* if the points in its stencil lie on both sides of the interface. We know that for a regular point, using the FDM stencil, the coefficients would be $\gamma_1 = \gamma_2 = \gamma_4 = \gamma_5 = \frac{\beta}{h^2}$ $\gamma_3 = \frac{-4\beta}{h^2}$

To find the coefficients for irregular points, we first need interface relations.

Interface relations derived from jump conditions and PDE are as follows:

$$u^+ = u^- + w \tag{6.6}$$

$$u_\xi{}^+ = \rho u_x i^- + \frac{v}{\beta^+} \tag{6.7}$$

$$u_\eta{}^+ = u_\eta{}^- + w^{'} \tag{6.8}$$

$$u_{\xi\xi}{}^+ = \Big(\frac{\beta_\xi{}^-}{\beta^+} - \chi^{''}\Big)u_\xi{}^- + \Big(\chi^{''} - \frac{\beta_\xi{}^+}{\beta^+}\Big)u_\xi{}^+ + \frac{\beta_\eta{}^-}{\beta^+}u_\eta{}^- - \frac{\beta_\eta{}^+}{\beta^+}u_\eta{}^+ + (\rho-1)u_{\eta\eta}{}^- + \rho u_{\xi\xi}{}^- - w^{''} + \frac{[f]}{\beta^+} + \frac{[\sigma]u^- + \sigma^+[u]}{\beta^+} \tag{6.9}$$

$$u_{\eta\eta}{}^+ = u_{\eta\eta}{}^- + (u_\xi{}^- - u_\xi{}^+)\chi^{''} + w^{''} \tag{6.10}$$

$$u_{\xi\eta}{}^+ = \frac{\beta_\eta{}^+}{\beta^+}u_\xi{}^+ + (u_\eta{}^+ - \rho u_\eta{}^-)\chi'' + \rho u_{\xi\eta}{}^- + \frac{v^{'}}{\beta^+} \tag{6.11}$$

where $\rho = \frac{\beta^-}{\beta^+}$ and $w^{'}, v^{'}, w^{''}, v^{''}$ are the first and second order surface derivatives of w, and v at (X, Y) on the interface.

IIM does not need any changes to be made to the grid in order to be used. For a Cartesian grid (x_i, y_j), $i = 0, 1, .., M$, $j = 0, 1, .., N$, the finite difference scheme is:

$$\sum_k^n \gamma_k U_{i+i_k, j+j_k} - \sigma_{ij}U_{ij} = f_{ij} + C_{ij} \tag{6.12}$$

The Taylor expansion of $u(x_{i+i+k}, y_{j+j_k})$ about (X, Y) in the local coordinate notation is:

$$u(x_{i+i_k}, y_{j+j_k}) = u(\xi_k, \eta_k) = u^\pm + \xi_k u_\xi{}^\pm + \eta_k u_\eta{}^\pm + \frac{1}{2}\xi_k{}^2 u_{\xi\xi}{}^\pm + \xi_k\eta_k u_{\xi\eta}{}^\pm + \frac{1}{2}\eta_k{}^2 u_{\eta\eta}{}^\pm + O(h^3) \tag{6.13}$$

In equation 3.13, the '+' and '-' are a representation of whether (ξ_k, η_k) lie on the '+' or '-' side of the interface. We expand the above equation and try to obtain the truncation error as a linear combination of values $u^\pm, u_\xi{}^\pm, u_\eta{}^\pm, u_{\xi\xi}{}^\pm, u_{\xi\eta}{}^\pm, u_{\eta\eta}{}^\pm$, leading to the following expression:

$$T_{ij} = a_1u^- + a_2u^+ + a_3u_\xi{}^- + a_4u_x i^+ + a_5u_\eta{}^- + a_6u_\eta{}^+ + a_7u_{\xi\xi}{}^- + a_8u_{\xi\xi}{}^+ + a_9u_{\eta\eta}{}^- + a_{10}u_{\eta\eta}{}^+ + a_{11}u_{\xi\eta}{}^- + a_{12}u_{\xi\eta}{}^+ - \sigma^-u^- - f^- - C_{ij} + max|\gamma_k|O(h^3) \tag{6.14}$$

The quantities $f^\pm$, $\sigma^\pm$, and $\beta^\pm$ are limiting values of the functions at (X,Y) from the '+' or '-' side of the interface. The coefficients a_i are independent of the PDE, jump conditions and other functional values. For convenience of notation, we defined two

index sets:

$K^{\pm} = k : (\xi_k, \eta_k)$ is on the " $\pm$ " side of the interface

Now, a_is are given by

$$a_1 = \sum_{k \in K_-} \gamma_k \tag{6.15}$$

$$a_2 = \sum_{k \in K_+} \gamma_k \tag{6.16}$$

$$a_3 = \sum_{k \in K_-} \xi_k \gamma_k \tag{6.17}$$

$$a_4 = \sum_{k \in K_+} \xi_k \gamma_k \tag{6.18}$$

$$a_5 = \sum_{k \in K_-} \eta_k \gamma_k \tag{6.19}$$

$$a_6 = \sum_{k \in K_+} \eta_k \gamma_k \tag{6.20}$$

$$a_7 = \sum_{k \in K_-} {\xi_k}^2 \gamma_k \tag{6.21}$$

$$a_8 = \sum_{k \in K_+} {\xi_k}^2 \gamma_k \tag{6.22}$$

$$a_9 = \sum_{k \in K_-} {\eta_k}^2 \gamma_k \tag{6.23}$$

$$a_{10} = \sum_{k \in K_+} {\eta_k}^2 \gamma_k \tag{6.24}$$

$$a_{11} = \sum_{k \in K_-} \xi_k \eta_k \gamma_k \tag{6.25}$$

$$a_{12} = \sum_{k \in K_+} \xi_k \eta_k \gamma_k \tag{6.26}$$

Interface relations 3.6 - 3.11 help in eliminating the quantities from one side, eliminate quantities from one side and collect the terms and substitute them in equation 3.14.

This leads us to the following relations:

$$a_1 + a_2 + a_8 \frac{[\sigma]}{\beta^+} = 0 \tag{6.27}$$

$$a_3 + \rho a_4 + a_8 \frac{{\beta_\xi}^- - \rho {\beta_\xi}^+ - [\beta]\chi''}{\beta^+} + a_{10} \frac{[\beta]\chi^{''}}{\beta^+} + a_{12} \frac{{\beta_\eta}^- - \rho {\beta_\eta}^+}{\beta^+} = {\beta_\xi}^- \tag{6.28}$$

$$a_5 + a_6 - a_8 \frac{[\beta_\eta}{\beta^+} + a_{12}(1-\rho)\chi^{''} = {\beta_\eta}^- \tag{6.29}$$

$$a_7 + a_8\rho = \beta^- \tag{6.30}$$

$$a_9 + a_{10} + a_8(\rho - 1) = \beta^- \tag{6.31}$$

$$a_{11} + a_{12}\rho = 0 \tag{6.32}$$

From these equations we will be able to find out γ_k using method of undetermined coefficients.

7. FORWARD PROBLEM

Taking the case of TE mode, the relevant equations are:

$$\nabla^2 \vec{E} + k^2 \vec{E} = 0 \tag{7.1}$$

$$\sigma_T = \sigma_P + \sigma_S \tag{7.2}$$

$${k_T}^2 = {k_S}^2 + {k_P}^2 \tag{7.3}$$

This leads us to

$$\nabla^2 E_P \vec{+} E_S + ({k_S}^2 + {k_P}^2) E_P \vec{+} E_S = 0 \tag{7.4}$$

Separating primary and secondary fields leads us to:

$$\nabla^2 \vec{E_S} + {k_T}^2 \vec{E_S} = {k_S}^2 \vec{E_P} \tag{7.5}$$

$$\nabla^2 \vec{E_P} + {k_P}^2 \vec{E_P} = 0 \tag{7.6}$$

The formulation of EM in the previous chapter is applicable here since the governing equations are elliptic. Because of the constraints imposed by the TE mode equation, the relations become much more simpler. The only term with discontinuity in this case is conductivity. Since it is only the secondary field that is affected by

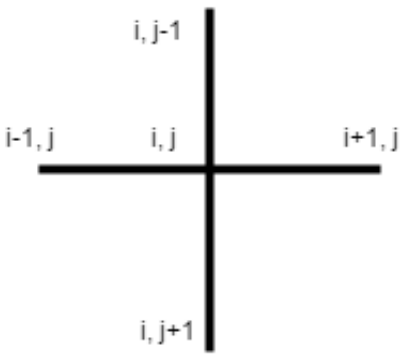

Figure 7.1: Points in FDM Stencil

anomaly. The formulation of EM can be represented in matrix form. First we need to calculate a_i. We can get this from the equation:

$$\begin{bmatrix} 1 & 1 & 0 & 0 & 0 & 0 & 0 & [k] & 0 & 0 & 0 & 0 \\ 0 & 0 & 1 & 1 & 0 & 0 & 0 & -\chi^{''} & 0 & \chi^{''} & 0 & 0 \\ 0 & 0 & 0 & 0 & 1 & 1 & 0 & 0 & 0 & 0 & 0 & 0 \\ 0 & 0 & 0 & 0 & 0 & 0 & 1 & 1 & 0 & 0 & 0 & 0 \\ 0 & 0 & 0 & 0 & 0 & 0 & 0 & 0 & 1 & 1 & 0 & 0 \\ 0 & 0 & 0 & 0 & 0 & 0 & 0 & 0 & 0 & 0 & 1 & 1 \end{bmatrix} \begin{bmatrix} a_1 \\ a_2 \\ a_3 \\ a_4 \\ a_5 \\ a_6 \\ a_7 \\ a_8 \\ a_9 \\ a_{10} \\ a_{11} \\ a_{12} \end{bmatrix} = \begin{bmatrix} 0 \\ 0 \\ 0 \\ 1 \\ 1 \\ 0 \end{bmatrix}$$

While solving for a_i the system needs to be regularized because of its proximity to singularity. Obtaining γ_k is the next step. The equation for this procedure changes with the position of the interface with respect to the stencil. First we consider the case when point 4 is on the right of the interface. In this case the equation becomes:

$$\begin{bmatrix} 1 & 1 & 1 & 0 & 1 \\ 0 & 0 & 0 & 1 & 0 \\ \xi_1 & \xi_2 & \xi_3 & 0 & \xi_5 \\ 0 & 0 & 0 & \xi_4 & 0 \\ \eta_1 & \eta_2 & \eta_3 & 0 & \eta_5 \\ 0 & 0 & 0 & \eta_4 & 0 \\ \xi_1 * \xi_1/2 & \xi_2 * \xi_2/2 & \xi_3 * \xi_3/2 & 0 & \xi_5 * \xi_5/2 \\ 0 & 0 & 0 & \xi_4 * \xi_4/2 & 0 \\ \eta_1 * \eta_1/2 & \eta_2 * \eta_2/2 & \eta_3 * \eta_3/2 & 0 & \eta_5 * \eta_5/2 \\ 0 & 0 & 0 & \eta_4 * \eta_4/2 & 0 \\ \xi_1 * \eta_1 & \xi_2 * \eta_2 & \xi_3 * \eta_3 & 0 & \xi_5 * \eta_5 \\ 0 & 0 & 0 & \xi_4 * \eta_4 & 0 \end{bmatrix} \begin{bmatrix} \gamma_1 \\ \gamma_2 \\ \gamma_3 \\ \gamma_4 \\ \gamma_5 \end{bmatrix} = \begin{bmatrix} a_1 \\ a_2 \\ a_3 \\ a_4 \\ a_5 \\ a_6 \\ a_7 \\ a_8 \\ a_9 \\ a_{10} \\ a_{11} \\ a_{12} \end{bmatrix}$$

When only point 2 is on the left of the interface, we have the following equation:

$$\begin{bmatrix} 0 & 1 & 0 & 0 & 0 \\ 1 & 0 & 1 & 1 & 1 \\ 0 & \xi_2 & 0 & 0 & 0 \\ \xi_1 & 0 & \xi_3 & \xi_4 & \xi_5 \\ 0 & \eta_2 & 0 & 0 & 0 \\ \eta_1 & 0 & \eta_3 & \eta_4 & \eta_5 \\ 0 & \xi_2 * \xi_2/2 & 0 & 0 & 0 \\ \xi_1 * \xi_1/2 & 0 & \xi_3 * \xi_3/2 & \xi_4 * \xi_4/2 & \xi_5 * \xi_5/2 \\ 0 & \eta_2 * \eta_2/2 & 0 & 0 & 0 \\ \eta_1 * \eta_1/2 & 0 & \eta_3 * \eta_3/2 & \eta_4 * \eta_4/2 & \eta_5 * \eta_5/2 \\ 0 & \xi_2 * \eta_2 & 0 & 0 & 0 \\ \xi_1 * \eta_1 & 0 & \xi_3 * \eta_3 & \xi_4 * \eta_4 & \xi_5 * \eta_5 \end{bmatrix} \begin{bmatrix} \gamma_1 \\ \gamma_2 \\ \gamma_3 \\ \gamma_4 \\ \gamma_5 \end{bmatrix} = \begin{bmatrix} a_1 \\ a_2 \\ a_3 \\ a_4 \\ a_5 \\ a_6 \\ a_7 \\ a_8 \\ a_9 \\ a_{10} \\ a_{11} \\ a_{12} \end{bmatrix}$$

When only point 1 is above the interface, we get

$$\begin{bmatrix} 0 & 1 & 1 & 1 & 1 \\ 1 & 0 & 0 & 0 & 0 \\ 0 & \xi_2 & \xi_3 & \xi_4 & \xi_5 \\ \xi_1 & 0 & 0 & 0 & 0 \\ 0 & \eta_2 & \eta_3 & \eta_4 & \eta_5 \\ \eta_1 & 0 & 0 & 0 & 0 \\ 0 & \xi_2 * \xi_2/2 & \xi_3 * \xi_3/2 & \xi_4 * \xi_4/2 & \xi_5 * \xi_5/2 \\ \xi_1 * \xi_1/2 & 0 & 0 & 0 & 0 \\ 0 & \eta_2 * \eta_2/2 & \eta_3 * \eta_3/2 & \eta_4 * \eta_4/2 & \eta_5 * \eta_5/2 \\ \eta_1 * \eta_1/2 & 0 & 0 & 0 & 0 \\ 0 & \xi_2 * \eta_2/2 & \xi_3 * \eta_3 & \xi_4 * \eta_4 & \xi_5 * \xi_5/2 \\ \xi_1 * \eta_1 & 0 & 0 & 0 & 0 \end{bmatrix} \begin{bmatrix} \gamma_1 \\ \gamma_2 \\ \gamma_3 \\ \gamma_4 \\ \gamma_5 \end{bmatrix} = \begin{bmatrix} a_1 \\ a_2 \\ a_3 \\ a_4 \\ a_5 \\ a_6 \\ a_7 \\ a_8 \\ a_9 \\ a_{10} \\ a_{11} \\ a_{12} \end{bmatrix}$$

Now, the only case that remains is when only point 5 is below the interface:

$$\begin{bmatrix} 0 & 0 & 0 & 0 & 1 \\ 1 & 1 & 1 & 1 & 0 \\ 0 & 0 & 0 & 0 & \xi_5 \\ \xi_1 & \xi_2 & \xi_3 & \xi_4 & 0 \\ 0 & 0 & 0 & 0 & \eta_5 \\ \eta_1 & \eta_2 & \eta_3 & \eta_4 & 0 \\ 0 & 0 & 0 & 0 & \xi_5 * \xi_5/2 \\ \xi_1 * \xi_1/2 & \xi_2 * \xi_2/2 & \xi_3 * \xi_3/2 & \xi_4 * \xi_4/2 & 0 \\ 0 & 0 & 0 & 0 & \eta_5 * \eta_5/2 \\ \eta_1 * \eta_1/2 & \eta_2 * \eta_2/2 & \eta_3 * \eta_3/2 & \eta_4 * \eta_4/2 & 0 \\ 0 & 0 & 0 & 0 & \xi_5 * \eta_5 \\ \xi_1 * \eta_1 & \xi_2 * \eta_2 & \xi_3 * \eta_3 & \xi_4 * \eta_4 & 0 \end{bmatrix} \begin{bmatrix} \gamma_1 \\ \gamma_2 \\ \gamma_3 \\ \gamma_4 \\ \gamma_5 \end{bmatrix} = \begin{bmatrix} a_1 \\ a_2 \\ a_3 \\ a_4 \\ a_5 \\ a_6 \\ a_7 \\ a_8 \\ a_9 \\ a_{10} \\ a_{11} \\ a_{12} \end{bmatrix}$$

8. INVERSE PROBLEM

The inverse-problem being a non-linear problem needs quasi-linearization. If the field is expanded about the initial guess parameter P^0, we obtain:

$$F_i(P) = F_i(P^0) + \sum_{j=1}^{n_p} \frac{\partial F_i}{\partial P_j}(P_j - {P_j}^0) + \frac{1}{2}\sum_{j=1}^{n_p}\sum_{k=1}^{n_p} \frac{\partial^2 F_i}{\partial P_j \partial P_k}(P_j - {P_j}^0)(P_k - {P_k}^0) + ... \quad (8.1)$$

where $i = 1, 2, .., n_o$, and $j = 1, 2, .., n_p$. Rewriting the above equation in matrix form

$$F(P) = F(P^0) + J.\Delta P + \frac{1}{2}\begin{bmatrix} \Delta P^T H_1 \Delta P \\ \Delta P^T H_2 \Delta P \\ \vdots \\ \Delta P^T H_{n_0} \Delta P \end{bmatrix} + ... \quad (8.2)$$

$F_i(P)$ is the response of the model P. J is the Jacobian matrix, and H is the Hessian matrix. It is safe to ignore higher order terms when using quasi-linearization, since the guess model is assumed to be close to true model. This reduces the above equation to

$$F(P) = F(P^0) + J.\Delta P \quad (8.3)$$

In another form,

$$J.\Delta P = \Delta R \quad (8.4)$$

,

where ΔR is the difference between $F(P)$, the observed response, and $F(P^0)$, the computed response, P^0 is the current parameter, ΔP is the correction to be applied, J is the Jacobian matrix, whose elements are the partial derivatives of data vector with respect to the parameters. J is also called sensitivity matrix, since it gives a measure of the effect on each data point because of change in a particular parameter. One can use ridge regression least square or minimum norm to solve for ΔP

$$\Delta P = (J^H J + \lambda^2 I)^{-1} J^H \Delta R$$

and

$$\Delta P = J^H (JJ^H + \lambda^2 I)^{-1} \Delta R$$

Using this we update the parameter as:

$$P = P^0 + \Delta P$$

The domain is discretized in blocks and inverted for position and resistivity. The Jacobian matrix is computed by perturbing the parameters slightly(1- 5 The updated parameters are used as initial guess for the next iteration. Convergence, in terms of improvement of parameters and level of fit, is checked after each iteration. Inversion stops either when convergence is reached, the change in RMS error is lesser than threshold or when a maximum number of iterations is reached.

9. RESULTS - IIM

9.1. Half-Space Model

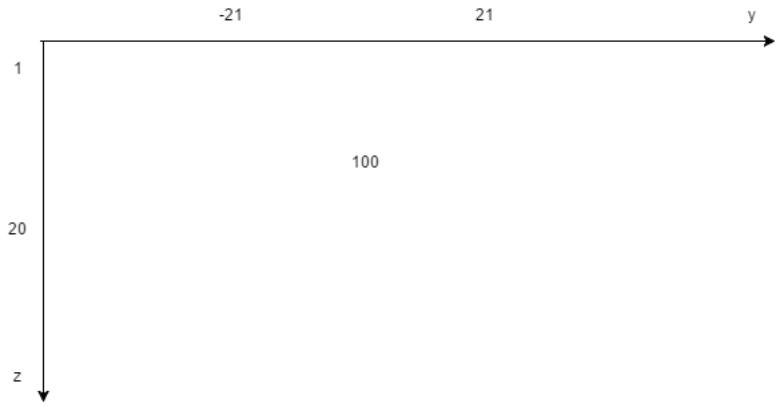

Figure 9.1: Half-space

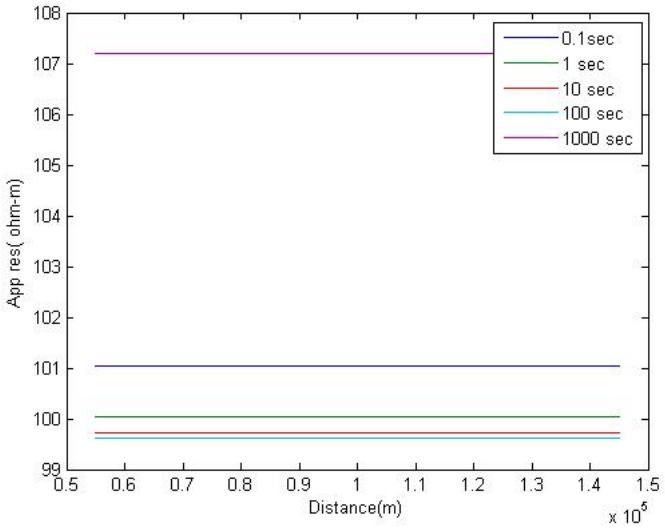

Figure 9.2: Half-space IIM

Table 9.1: Errors - Half Space

Time Period(sec)	RMS Error(%)	Average Error(%)	Maximum Error(%)
0.1	0.5712	0.0724	0.0724
1	0.0953	0.0303	0.0316
10	0.0256	0.0159	0.019
100	0.0017	0.0042	0.0042
1000	1.1063	0.1069	0.1069

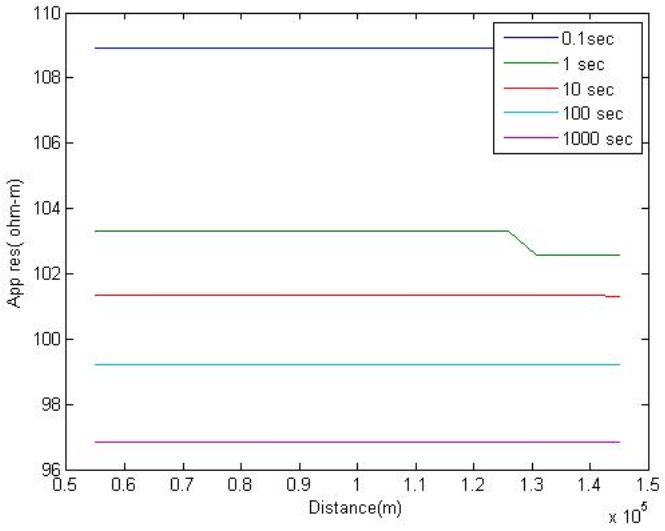

Figure 9.3: Half-space IIM

9.2. Single Conductive Anomaly

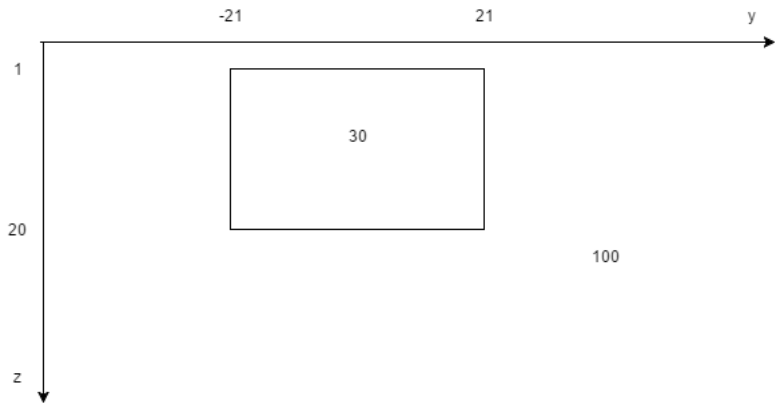

Figure 9.4: Single Conductive Anomaly

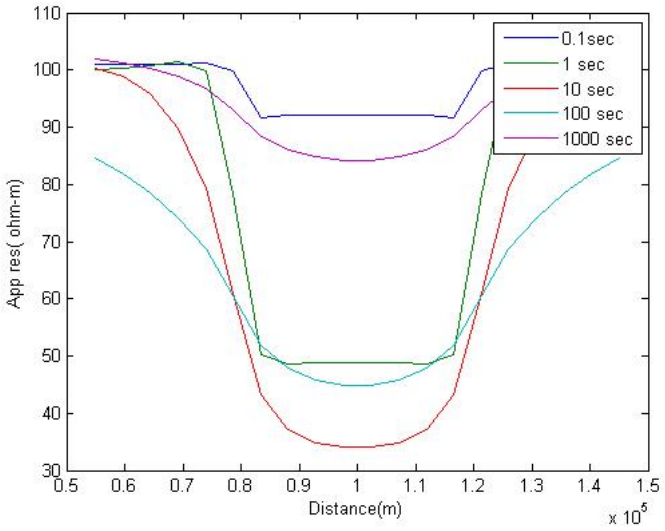

Figure 9.5: Single Conductive Heterogeneity IIM

Table 9.2: Errors - Single Conductive Anomaly

Time Period(sec)	RMS Error(%)	Average Error(%)	Maximum Error(%)
0.1	3.1598e-01	5.2856e-02	7.2233e-02
1	1.8810e-01	1.9533e-02	9.1792e-02
10	5.0440e-02	1.2578e-02	8.0233e-02
100	4.3556e-02	2.4920e-02	4.8664e-02
1000	1.2944e-01	3.7709e-02	4.5933e-02

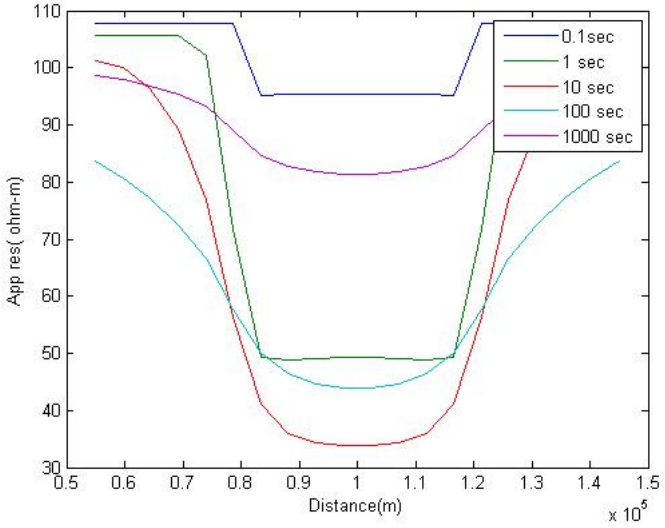

Figure 9.6: Single Conductive Heterogeneity FDM

9.3. Single Resistive Anomaly

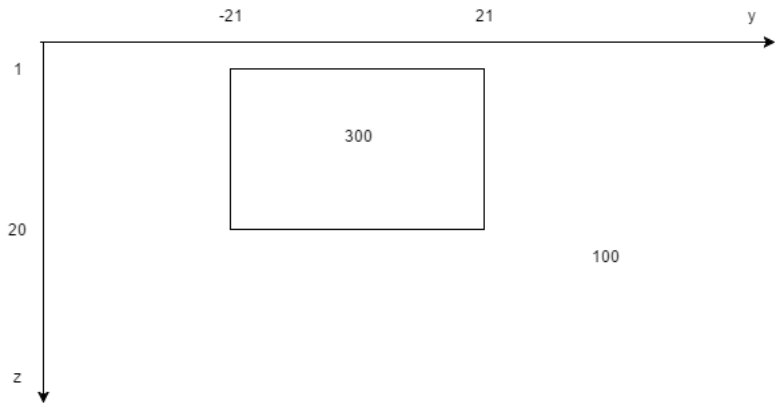

Figure 9.7: Single Resistive Anomaly

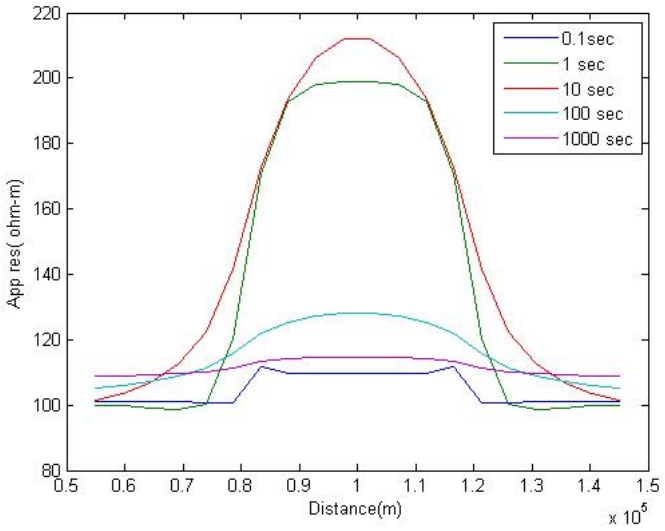

Figure 9.8: Single Resistive Heterogeneity IIM

Table 9.3: Errors - Single Resistive Anomaly

Time Period(sec)	RMS Error(%)	Average Error(%)	Maximum Error(%)
0.1	2.6923e+00	1.4552e-01	1.6756e-01
1	9.2553e-01	6.3987e-02	1.1678e-01
10	4.1612e-01	4.5768e-02	6.8909e-02
100	3.0041e-03	3.7229e-03	1.0890e-02
1000	1.1258e+00	1.0563e-01	1.0718e-01

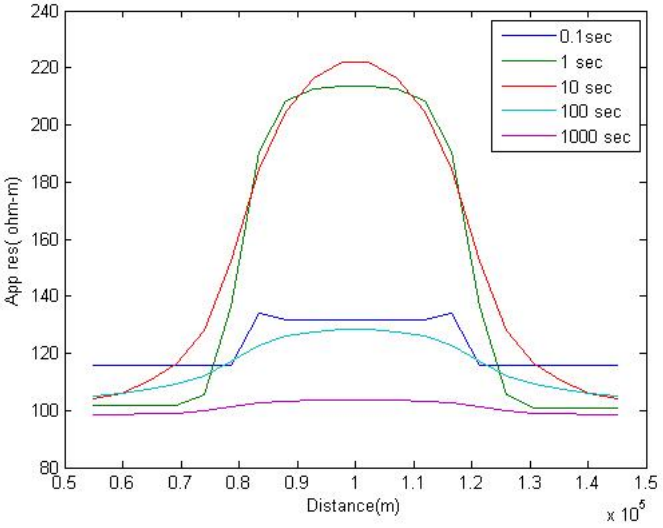

Figure 9.9: Single Resistive Heterogeneity FDM

9.4. One Conductive, One Resistive Anomaly

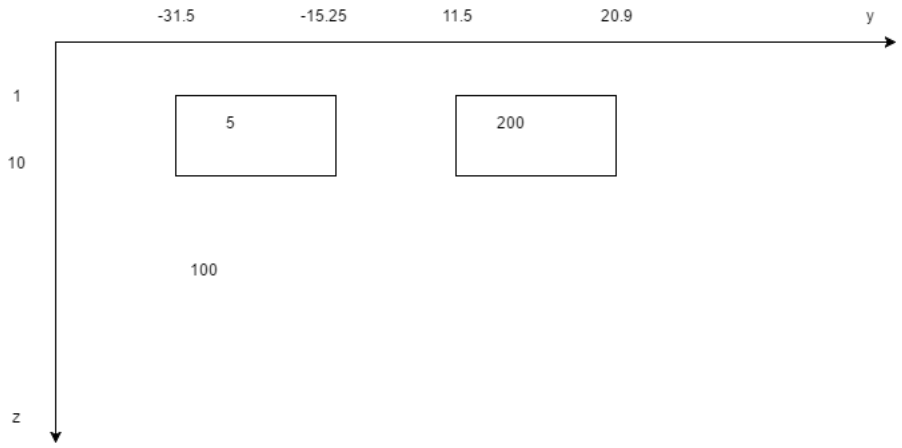

Figure 9.10: One Conductive, One Resistive Anomaly

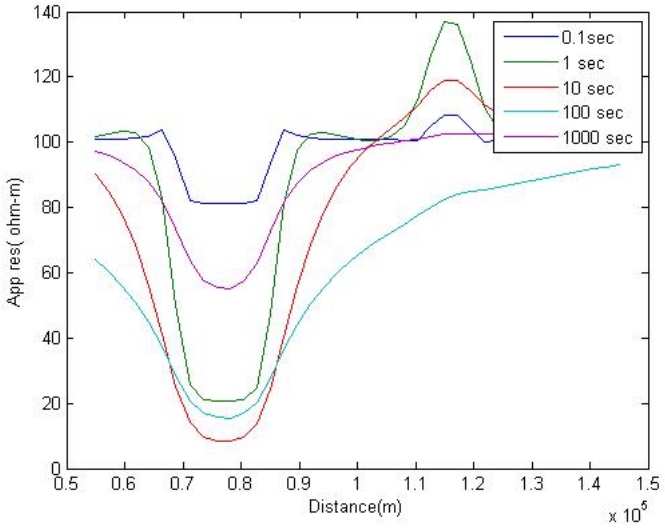

Figure 9.11: One conductive anomaly, and one resistive anomaly IIM

Table 9.4: Errors - One conductive anomaly, and one resistive anomaly

Time Period(sec)	RMS Error(%)	Average Error(%)	Maximum Error(%)
0.1	1.4141e-01	7.2764e-03	1.6603e-01
1	2.8297e-01	1.1087e-02	6.9286e-01
10	1.3280e-01	1.2517e-02	5.1033e-01
100	4.8160e-01	8.1809e-02	4.3886e-01
1000	5.2506e-01	7.6053e-02	2.0387e-01

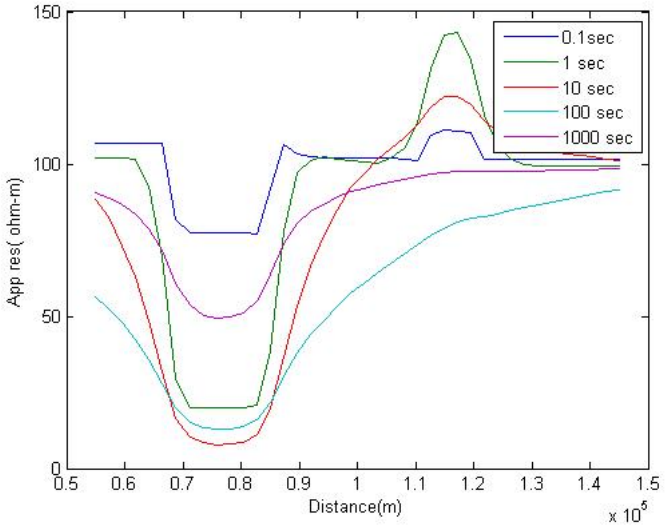

Figure 9.12: One conductive anomaly, and one resistive anomaly FDM

9.5. One Resistive, One Conductive Anomaly

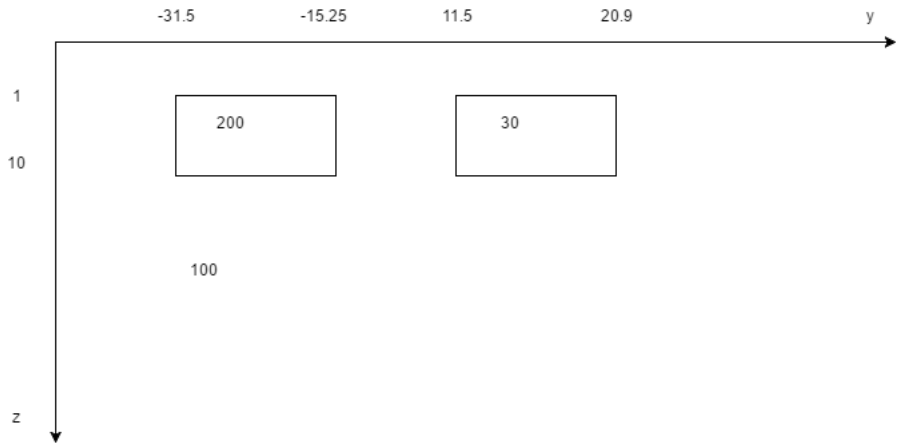

Figure 9.13: One Resistive, One Conductive Anomaly

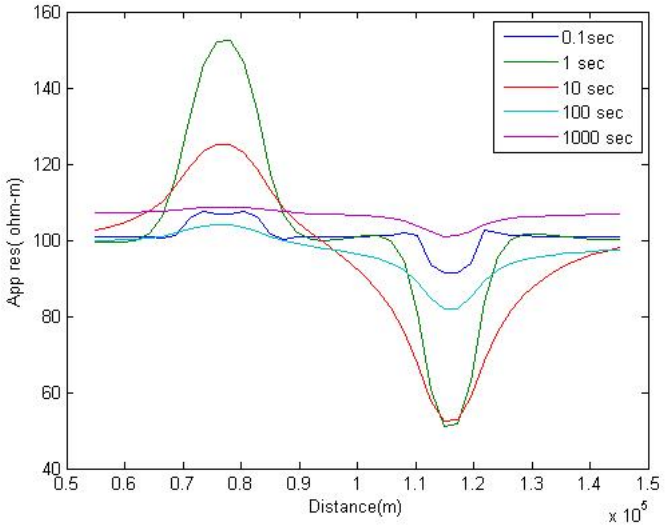

Figure 9.14: One resistive anomaly, and one conductive anomaly IIM

Table 9.5: Errors - One resistive anomaly, and one conductive anomaly

Time Period(sec)	RMS Error(%)	Average Error(%)	Maximum Error(%)
0.1	1.8958e+00	1.2066e-01	1.8177e-01
1	6.3574e-01	5.3758e-02	1.3746e-01
10	1.6068e-01	1.5952e-02	1.0700e-01
100	2.4844e-02	1.0712e-02	4.9317e-02
1000	1.0158e-01	3.1234e-02	4.2678e-02

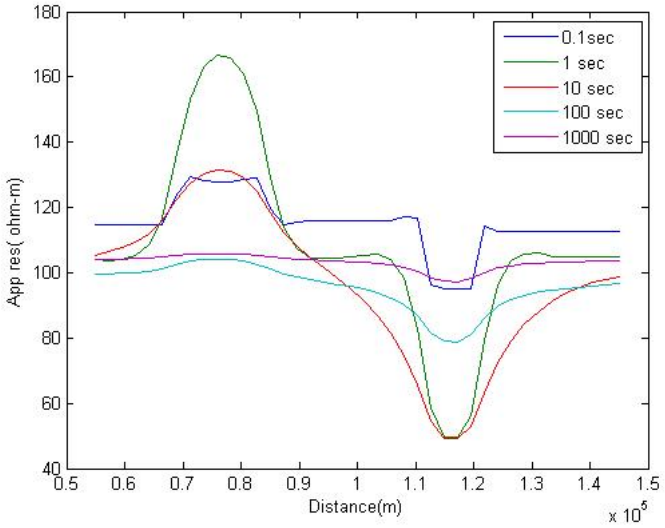

Figure 9.15: One resistive anomaly, and one conductive anomaly FDM

It can be seen from the figures that the results from IIM match the results of conventional FDM within reasonable error bounds. The computational time was also found to be less than or equal to conventional method in most cases.

Part II

Crustal Deformation Studies in Antarctica using GPS Data

10. INTRODUCTION TO GPS

GPS stands for NAVigation System with Time and Ranging Global Positioning System. The system has three segments:

- Space: Satellites
- Control: Stations spread across the Earth, near the equator to control the satellites.
- User: Any user sending and receiving GPS signals. We fall in this category.

The positioning of the satellite is such that at any given point on Earth, at any given instant there are at least four satellites visible above the 15deg cutoff angle. The satellites broadcast two carrier waves in the L-band constantly, which are derived from a fundamental frequency, derived from a fundamental frequency generated by an atomic clock onboard the satellite. L1 frequency is 1575.42MHz, while the L2 frequency is 1227.60MHz.

Getting position using GPS is based on measuring the distance between the GPS receiver on Earth and satellite. To get the position at least three satellites are needed. The receiver would be located at the intersection of three spheres of the radii the same as the distance between the receiver and the satellites. The distances would have to be calculated as we can only know the pseudoranges and the time at which the signals arrived can be determined. There are four unknowns to be determined position (X, Y, Z) and time of travel. The four unknowns can be achieved from four equations, by using at least four satellites.

11. INTRODUCTION TO ANTARCTICA

The Antarctic Plate is a tectonic plate containing the continent of Antarctica and extending outward under the surrounding oceans. After breakup from Gondwana, the southern part of the supercontinent Pangea, the Antarctic plate began moving the continent of Antarctica south to its present isolated location causing the continent to develop a much colder climate. The Antarctic Plate is bounded almost entirely by extensional mid-ocean ridge systems. The adjoining plates are the Nazca Plate, the South American Plate, the African Plate, the Indo-Australian Plate, the Pacific Plate, and, across a transform boundary, the Scotia Plate. The Antarctic plate movement is estimated at least 1 cm/ year towards the Atlantic Ocean.

11.1. MAITRI

Maitri is located in Schirmacher Oasis. The co-ordinates of the station are $70^{\mathrm{deg}}46'00"S$, $11^{\mathrm{deg}}43'56"E$. The oasis is located between the edge of the Antarctic Ice Sheet and the Novolazarevskaya Nivl Ice Shelf. The approximately 100 m high plateau of the Schirmacher Oasis is a barrier to the northwards running ice stream. On the northern edge of the oasis are so-called epishelf lakes, bays separated from the ocean, which are connected with the ocean underneath the surface of the ice. Thus, tidal effects can be observed in the lakes. The epishelf lakes can contain either mere freshwater or saltwater which is overlaid by freshwater. The Antarctic Ice Sheet, southwards of the Schirmacher Oasis, reaches heights of 1500 m. The nunataks Skaly Instituta Geologii Arktiki (Skaly IGA) and Basisny-Kit protrude from the ice sheet. Between the offshore ice sheet and the Wegener Ice Sheet Plateau are the Wohlthat Mountains.

12. TOOLS USED FOR PROCESSING

GAMIT is collection of programs to process phase data to estimate three-dimensional relative positions of ground stations and satellite orbits, atmospheric zenith delays, and earth orientation parameters.

GLOBK is a Kalman filter whose primary purpose is to combine various geodetic solutions such as GPS, VLBI, and SLR experiments. It accepts as data, or "quasi-observations" the estimates and covariance matricies for station coordinates, earth-orientation parameters, orbital parameters, and source positions generated from the analysis of the primary observations. The input solutions are generally performed with loose a priori uncertainties assigned to all global parameters, so that constraints can be uniformly applied in the combined solution.

The basic outline of steps followed during processing of GPS data is:

1. Get the orbital files, i.e., generate reference orbit for satellites.
2. Prepare the data for processing.
3. Compute residuals and partial derivatives of the observations
4. Detect outliers or breaks (cycle-slips) in the data
5. Perform a least square analysis to estimate the positions of a set of stations

The steps followed with GAMIT are:

1. Put all files in *rinex* directory in your project directory.
2. Run *sh_setup* to set up the *tables* directory. The parameters needed is the year.
3. Get data files for IGS stations.
4. Set up your experiment by editing *sites.defaults* file.

5. Get G files, which are orbital files.
6. Get ephemeris files.
7. Prepare l-file, which includes apriori position information about the sites.
8. Prepare and edit *sittbl.* for site-specific processing parameters.
9. Prepare and edit *settbl.* for editing relevant parameters.
10. Run GAMIT.
11. Evaluate the quality of the results. This gives us loosely constrained solution.
12. Copy the h-files to *glbf* directory.
13. Prepare the *globk_comb* and *glorg_comb* cmd files.
14. Run *sh_glred* to obtain better constrained solutions.
15. Run GLOBK to obtain velocity estimates.

13. ERROR SOURCES IN GPS

GPS is not an error-free system, and there are several sources which can induce errors in measurements. The most important ones being:

1. Ionospheric and Atmospheric Delays: While passin through the ionosphere and atmosphere, a delay is introduced. This delay is not constant, and depends on satellite elevation, density of the ionosphere, and humidity. If the satellite is at a low elevation, it will have to travel a longer distance to reach the receiver, thus increasing the delay introduced. Higher elevation satellites will have lower ionospheric error. Denser the ionosphere, higher is the error introduced. During the day, the ionospheric density(Total Electron Content) increases, while at night the Sun doesn't affect the ionosphere. Error due to ionosphere is lesser during the day than at night. Solar flares also introduce an error in GPS and must be taken into account. The simplest way to mitigate ionospheric error is taking an average of the effect of velocity reduction of signal. However, average conditions do not occur all the time, thus rendering this solution as not an optimal one. Alternatively, one can use two frequencies, and compare the difference in their arrival times. The error introduced by ionosphere would be in proportion to the time difference, since signal slows down inversely proportional to frequency. Water vapour content in the atmosphere also introduces errors in GPS data, but it can be corrected using atmospheric models.

2. Satellite and Receiver Clock Errors: Even though the clocks onboard the satellites are very accurate, sometimes error creeps in and they drift from the correct time. This error in time can affect the accuracy of the position.

3. Multipath Errors: Multipath occurs due to the presence of highly reflective bodies near the receiver. Examples of such bodies are buildings and lakes. It is

for this reason that a GPS antenna should not be placed in a valley. This error is best avoided by placing the antenna in a place away from high buildings and reflective bodies.

4. Dilution of Precision: This is a representative of how well distributed the satellites are in the sky. If the satellites are well spaced then the uncertainty in position will be less. The uncertainty is the overlapping range of the two satellites. If the satellites are close then their overlap increases, leading to higher uncertainty. The types of DOP commonly used are:

    - VDOP - Veritcal Dilution of Precision gives the accuracy degradation in vertical direction.
    - HDOP - Horizontal Dilution of Precision gives the accuracy degradation in horizontal direction.
    - PDOP - Positional Dilution of Precision gives the accuracy degradation in 3D position.
    - GDOP - Geometrical Dilution of Precision gives the accuracy degradation in 3D position and time. It is the most comprehensive of all DOP quantities.

    To minimize error, it is best to take several well spaced satellites, and ignore the ones below 15^{deg} below the horizon

The following diagrams show the error at various sites taken for this study. It is seen that the errors are within limits, and were corrected.

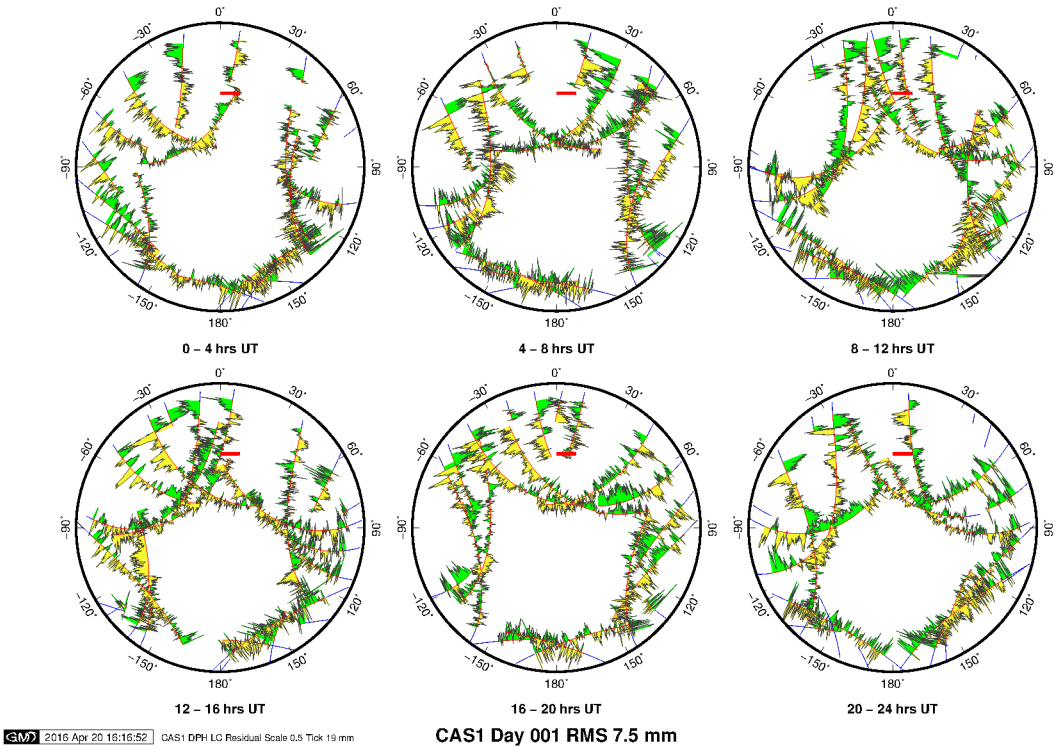

Figure 13.1: Sky plot at CAS1

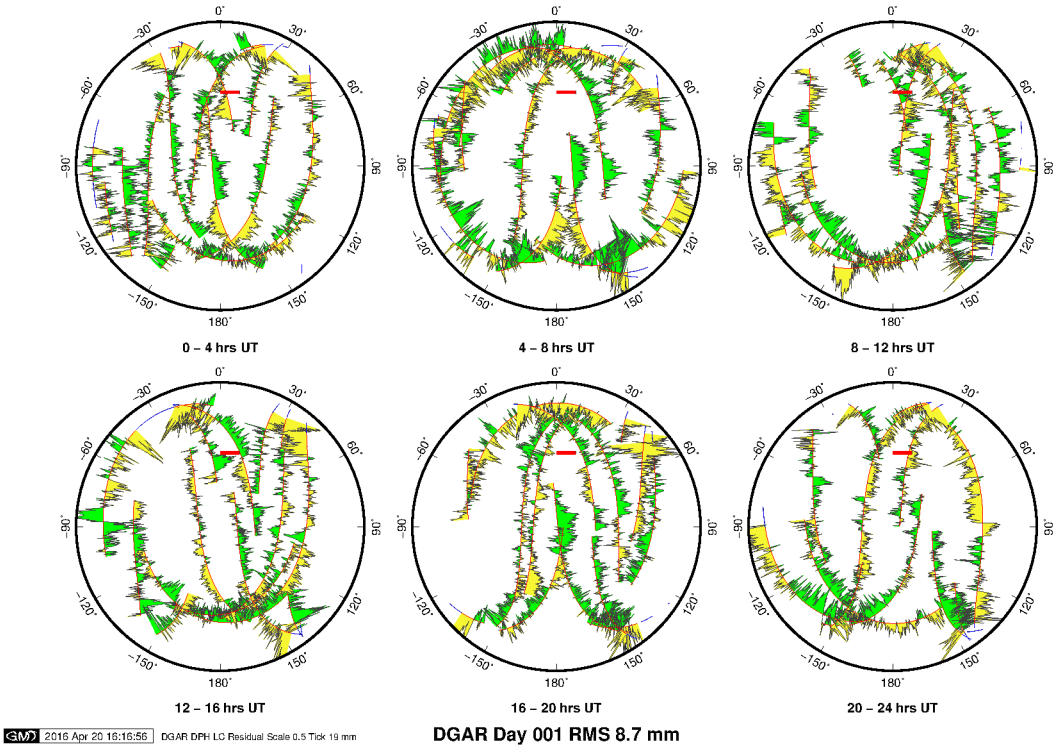

Figure 13.2: Sky plot at DGAR

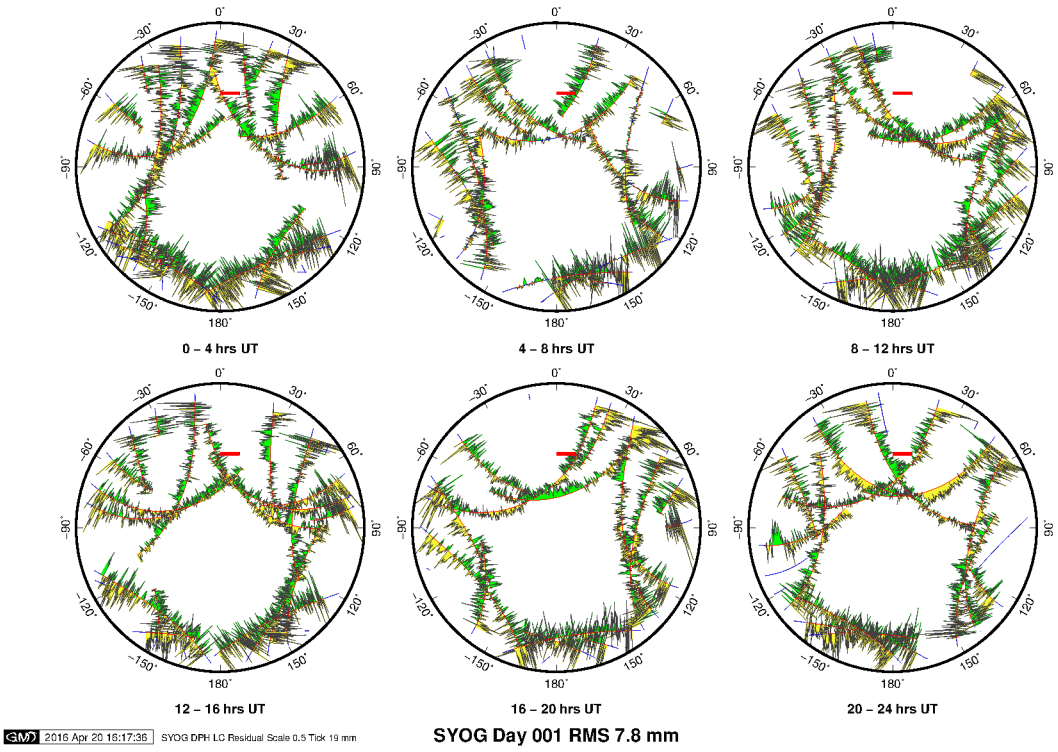

Figure 13.3: Sky plot at SYOG

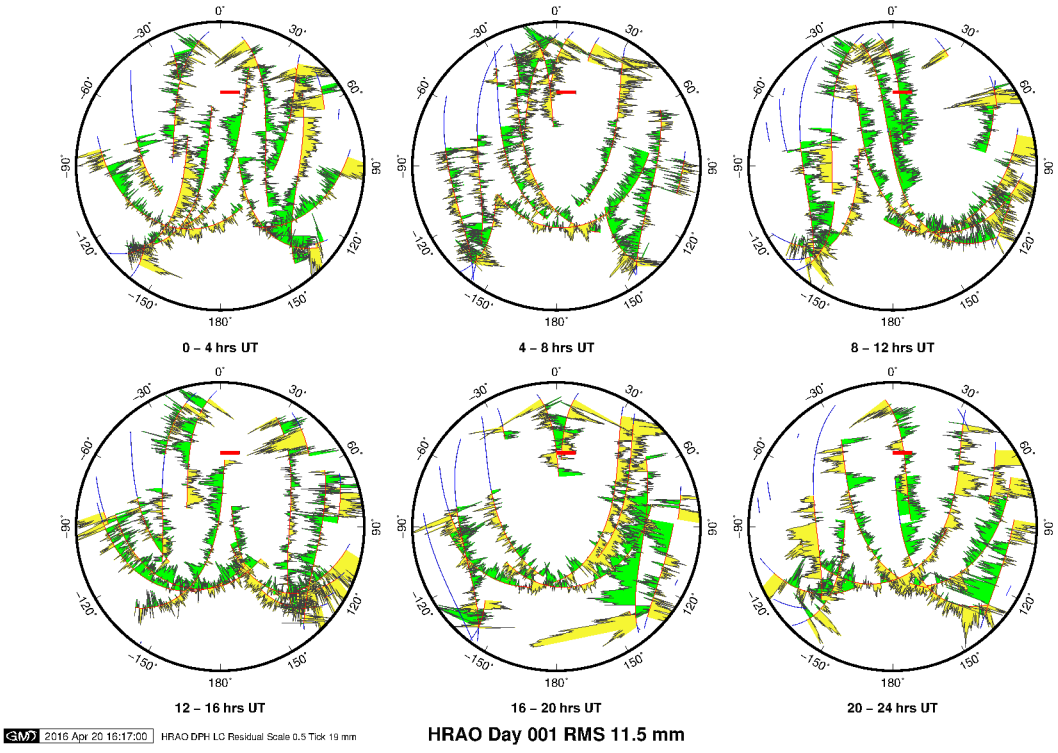

Figure 13.4: Sky plot at HRAO

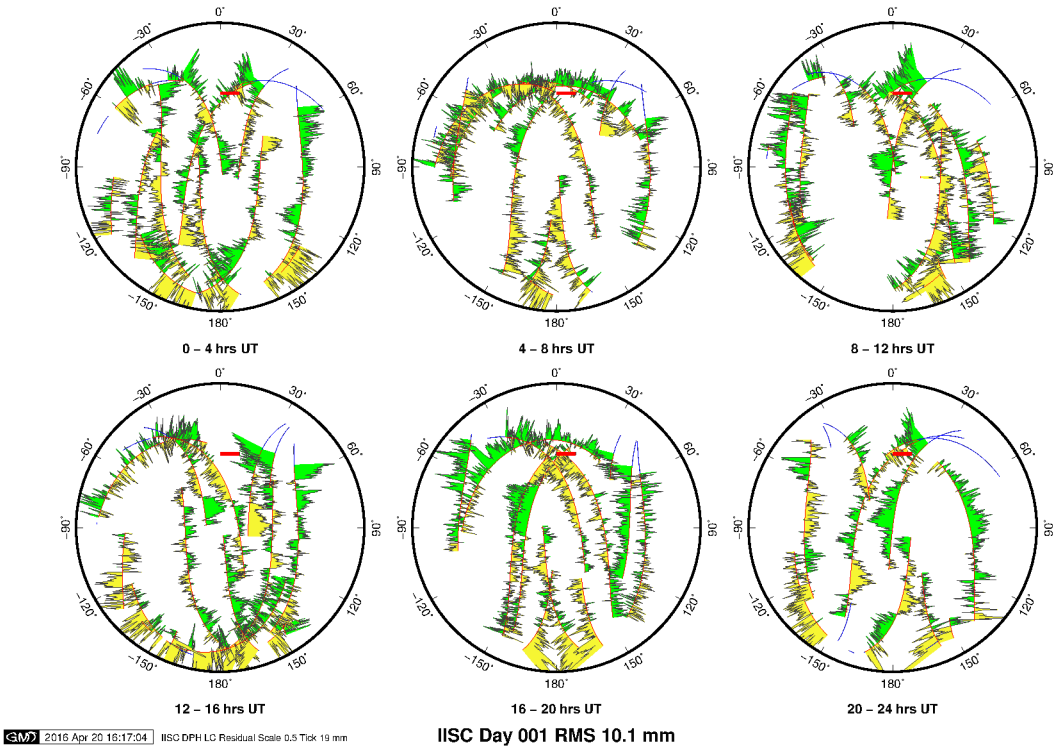

Figure 13.5: Sky plot at IISC

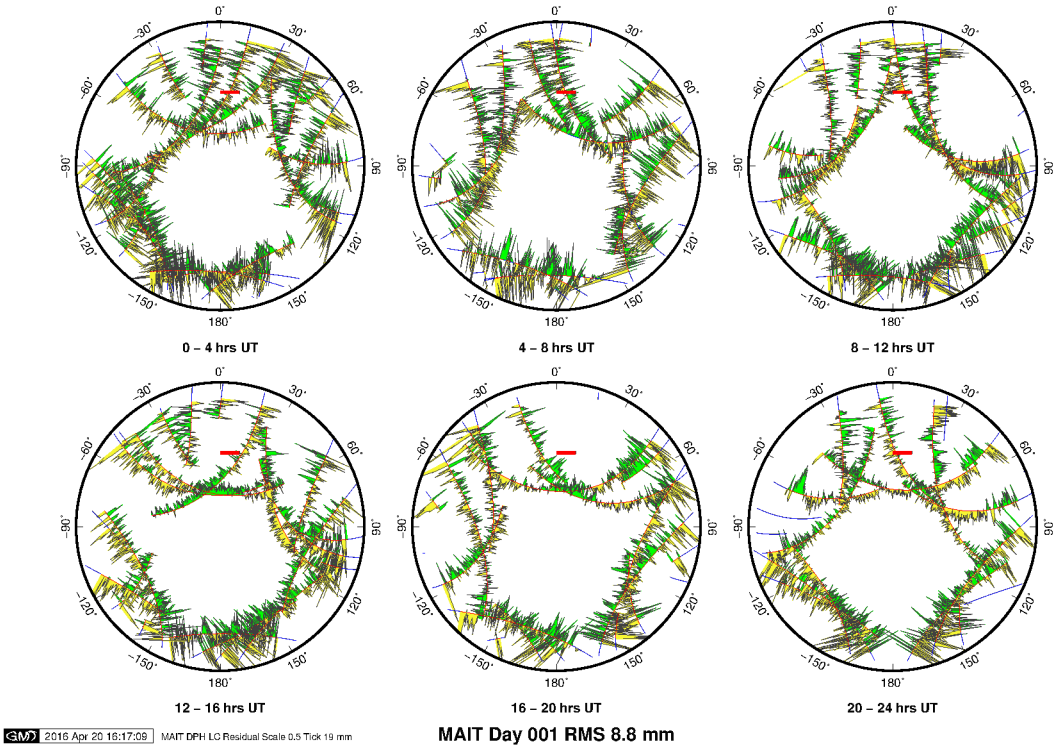

Figure 13.6: Sky plot at MAIT

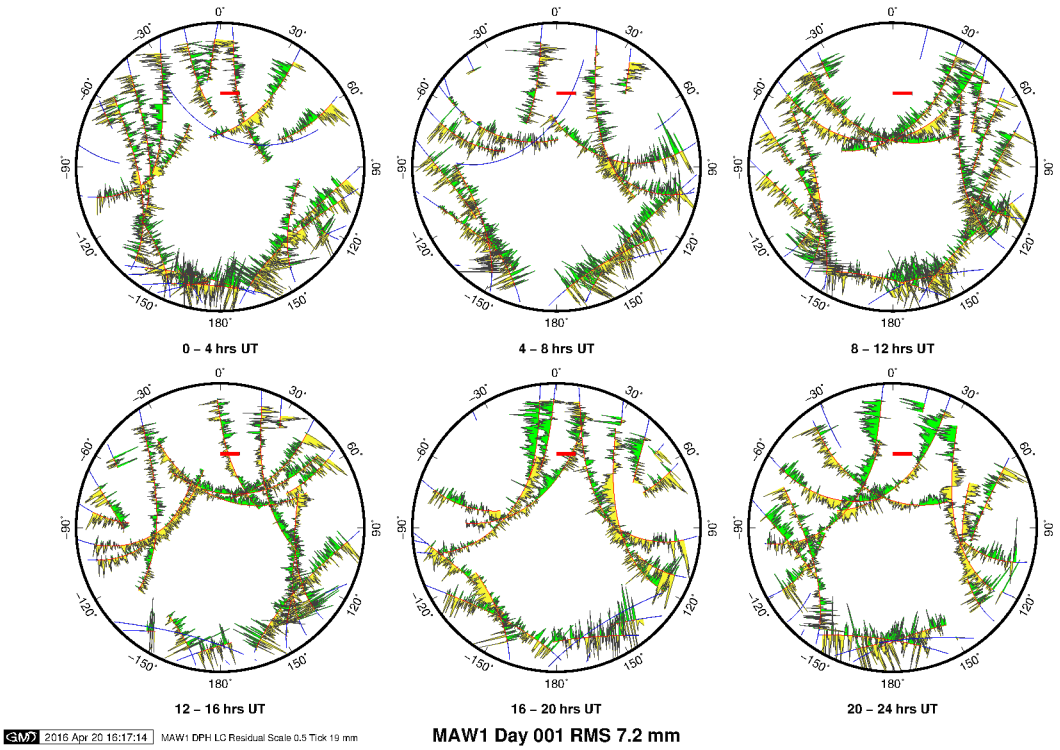

Figure 13.7: Sky plot at MAW1

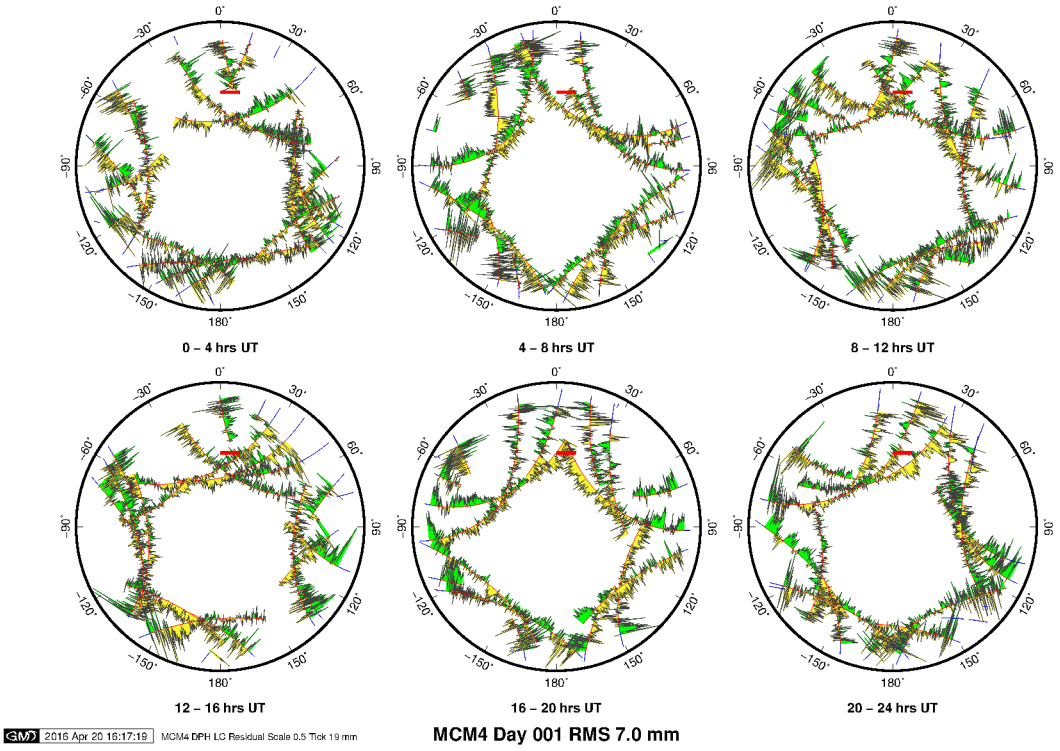

Figure 13.8: Sky plot at MCM4

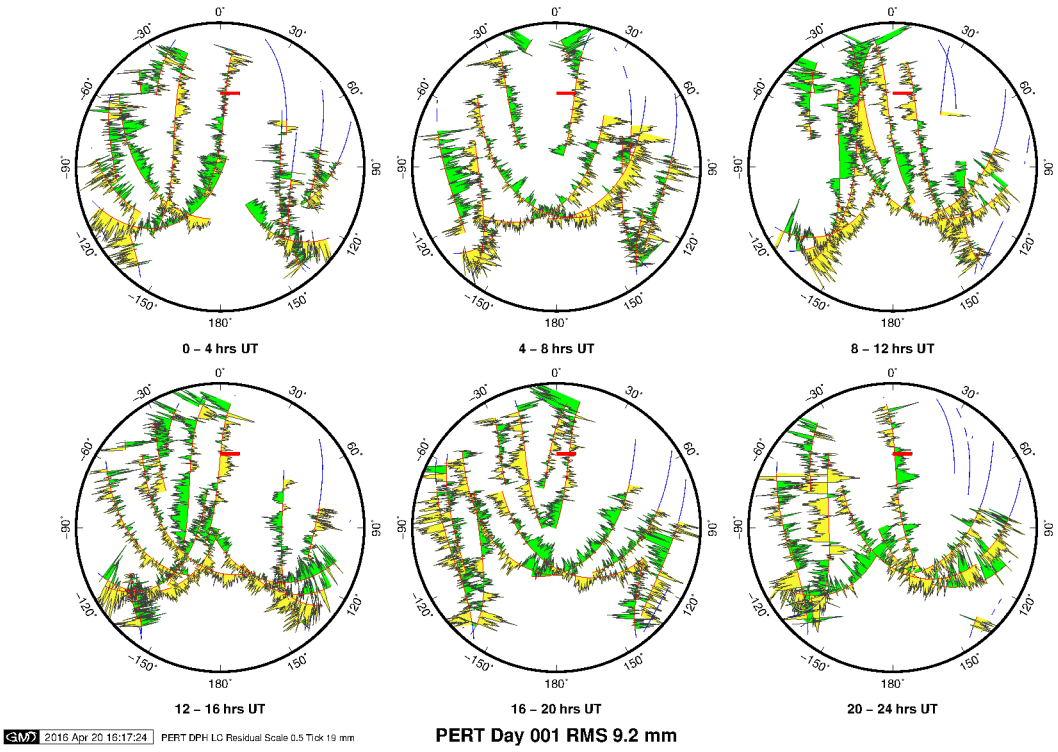

Figure 13.9: Sky plot at PERT

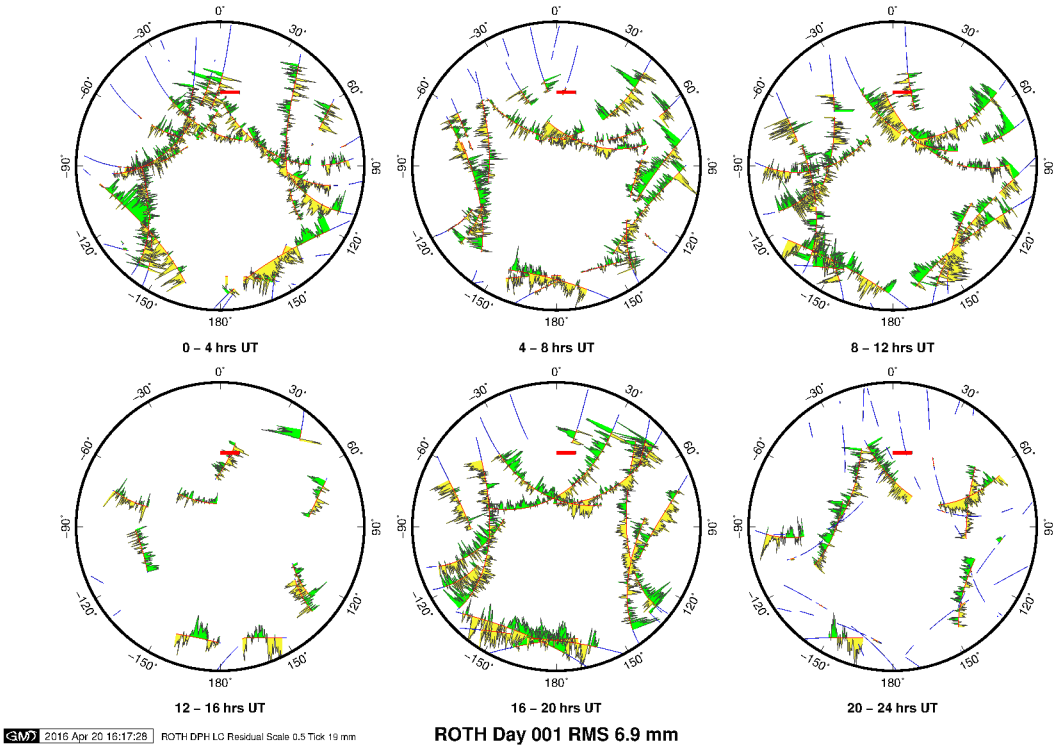

Figure 13.10: Sky plot at ROTH

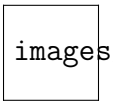

Figure 13.11: Sky plot at SEY1

14. VELOCITY ESTIMATE

Presented below are first, the time series for various stations during January 2016, and then the comparison of January 2016 with January 2015. The site Maitri is shown moving East at 2.46 mm/year, North at 6.68mm/year. Rate, adjustment, and error are given in mm/year.

Table 14.1: Velocity Estimates

E Rate	N Rate	E adj	N Adj.	E+-	N+-	RHO	H Rate	H adj.	H+-	SITE
12.34	-3.32	-1.80	-13.54	0.38	0.62	-0.039	-8.79	-14.61	2.36	ROTH
10.97	-22.27	1.03	-10.70	0.40	0.40	0.011	34.44	36.03	1.88	MCM4
8.13	-14.95	-0.23	-3.53	0.56	0.64	-0.030	-45.53	-45.39	2.31	DUM1
3.89	-13.61	2.30	-3.60	0.47	0.51	-0.039	-4.42	0.55	1.54	CAS1
48.99	55.56	9.85	-2.57	0.80	0.78	0.018	-59.70	-58.03	2.03	PERT
77.60	110.21	31.91	59.36	24.01	16.15	0.005	-250.63	-251.35	70.50	COCO
38.82	18.86	-3.02	-16.65	0.17	0.38	-0.075	-54.37	-55.09	2.92	IISC
0.15	37.39	-46.38	4.72	18.08	13.09	-0.042	-49.03	-50.47	56.46	DGAR
6.38	0.89	1.47	3.33	0.46	0.54	-0.027	-84.63	-84.51	1.88	KERG
2.46	6.68	2.46	6.68	0.54	0.54	-0.004	-58.07	-58.07	1.86	MAIT

Presented below is a pictorial representation of velocity estimates:

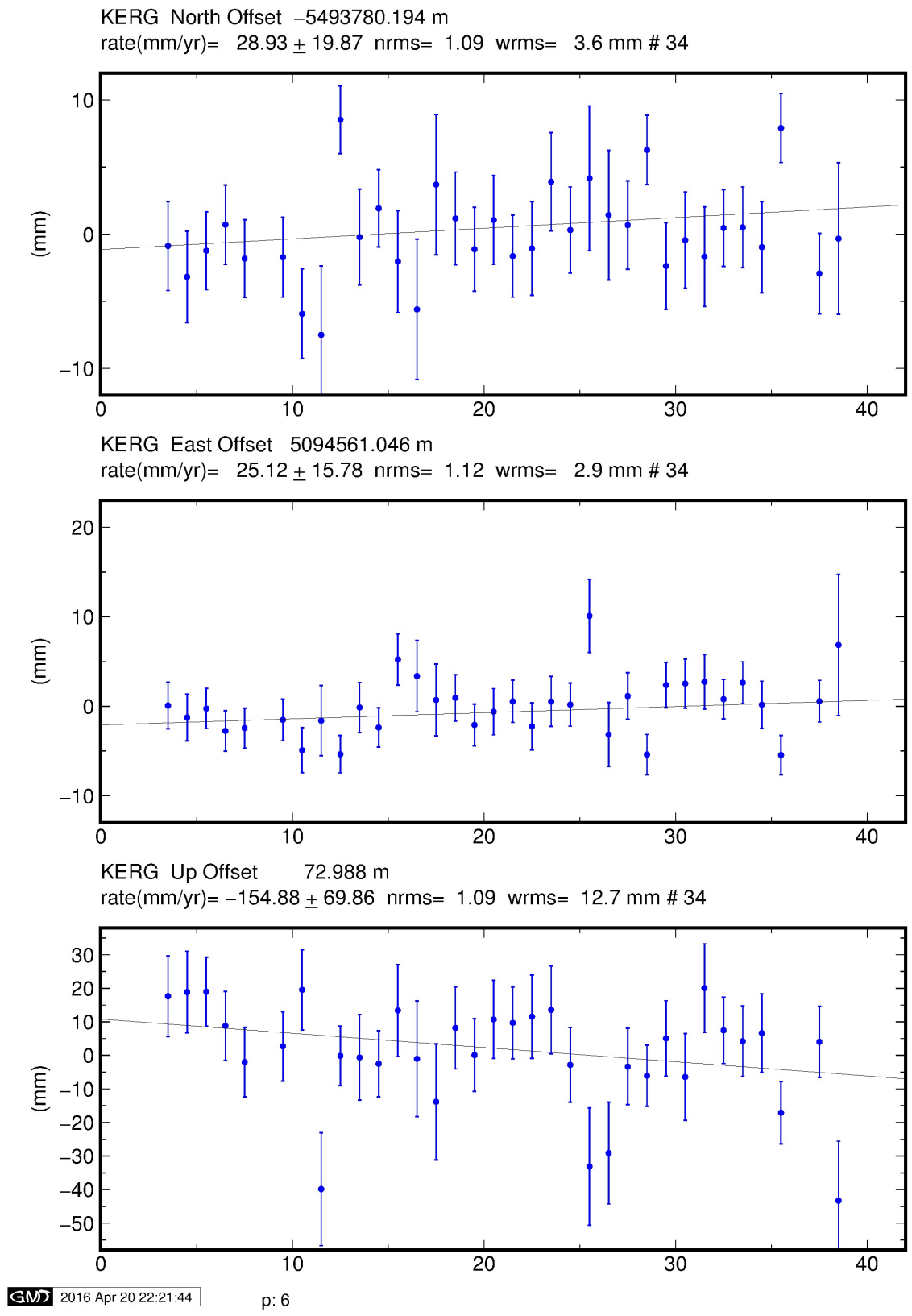

Figure 14.1: Time series for KERG, January 2016

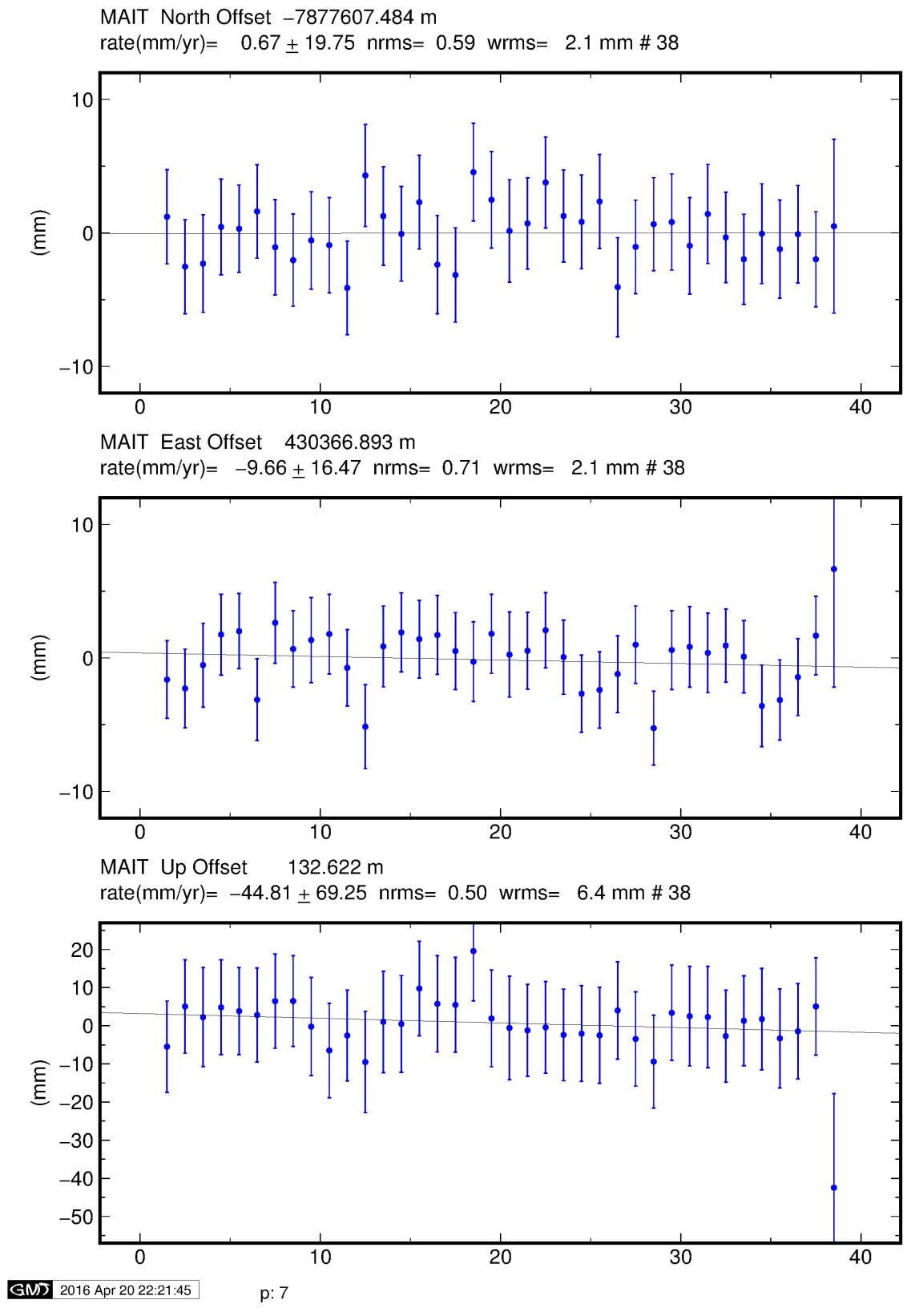

Figure 14.2: Time series for MAIT, January 2016

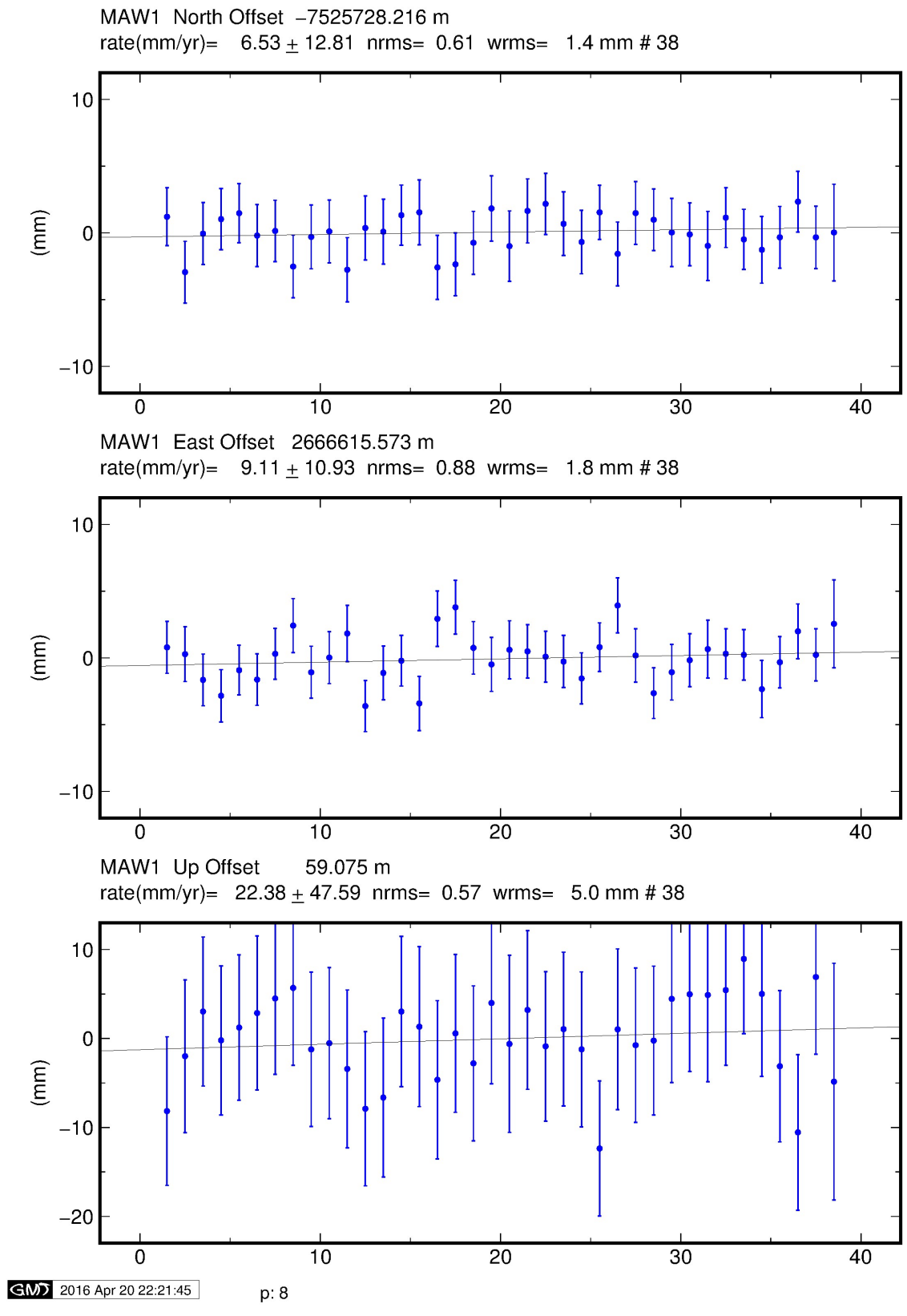

Figure 14.3: Time series for MAW1, January 2016

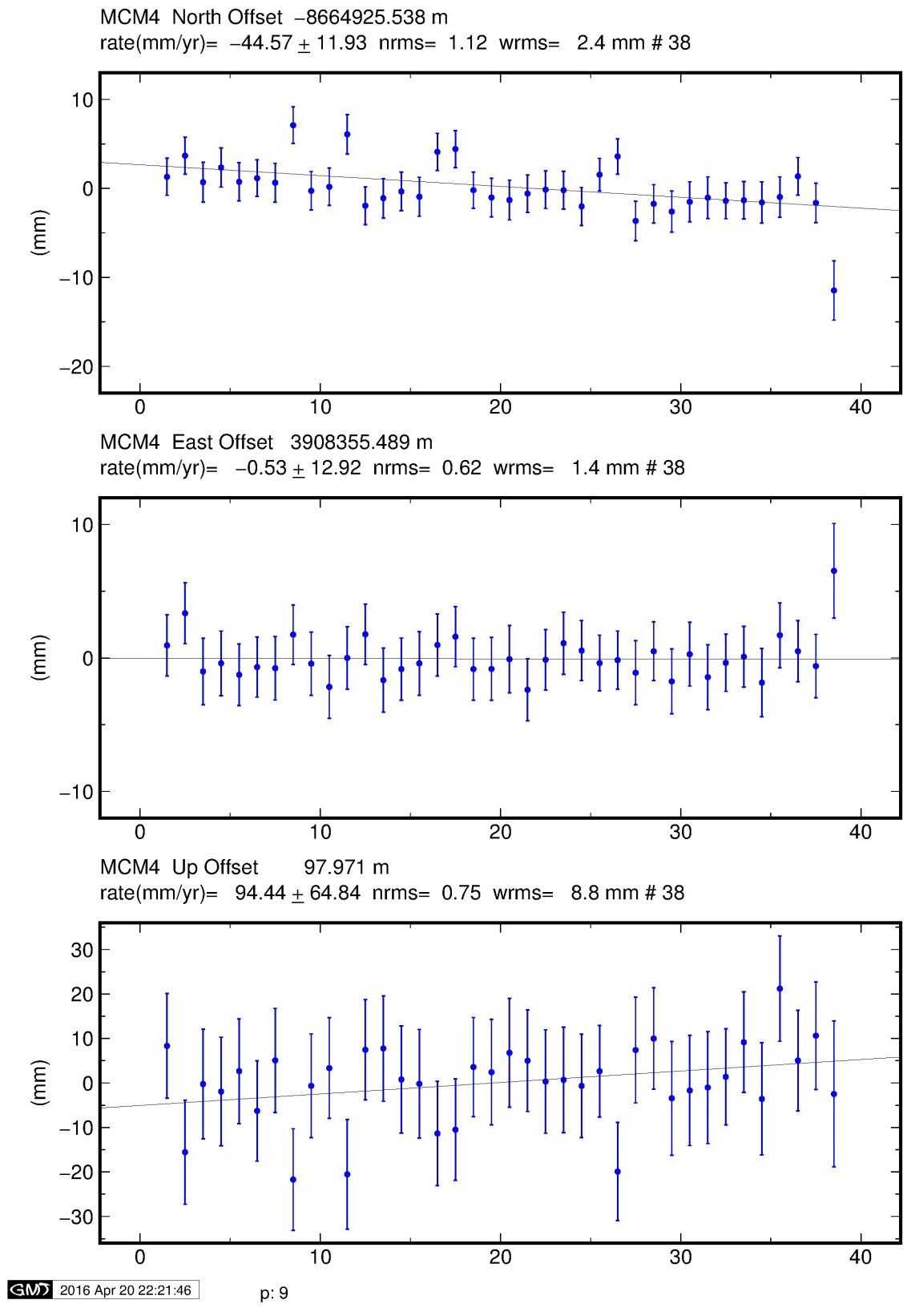

Figure 14.4: Time series for mcm41, January 2016

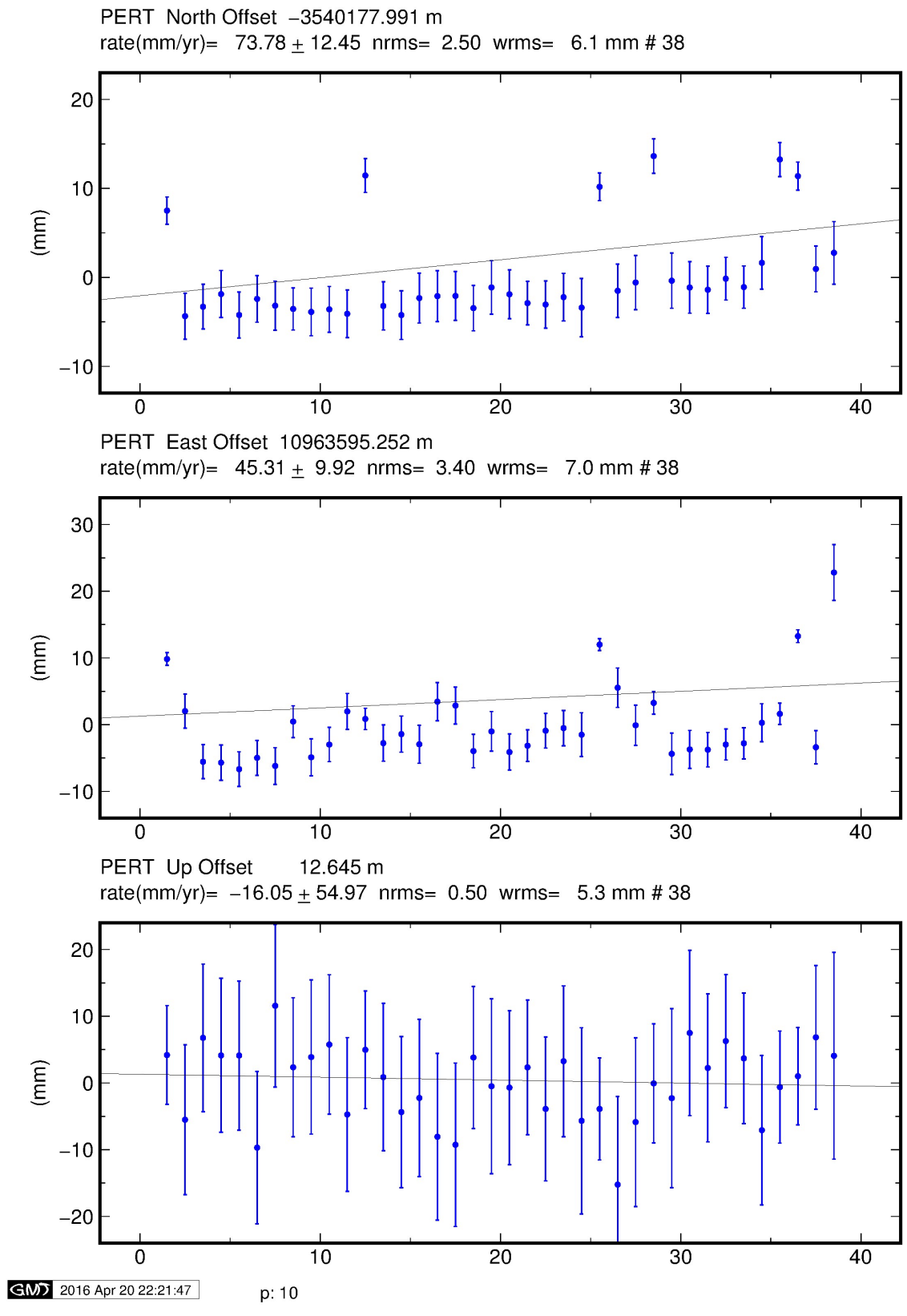

Figure 14.5: Time series for PERT, January 2016

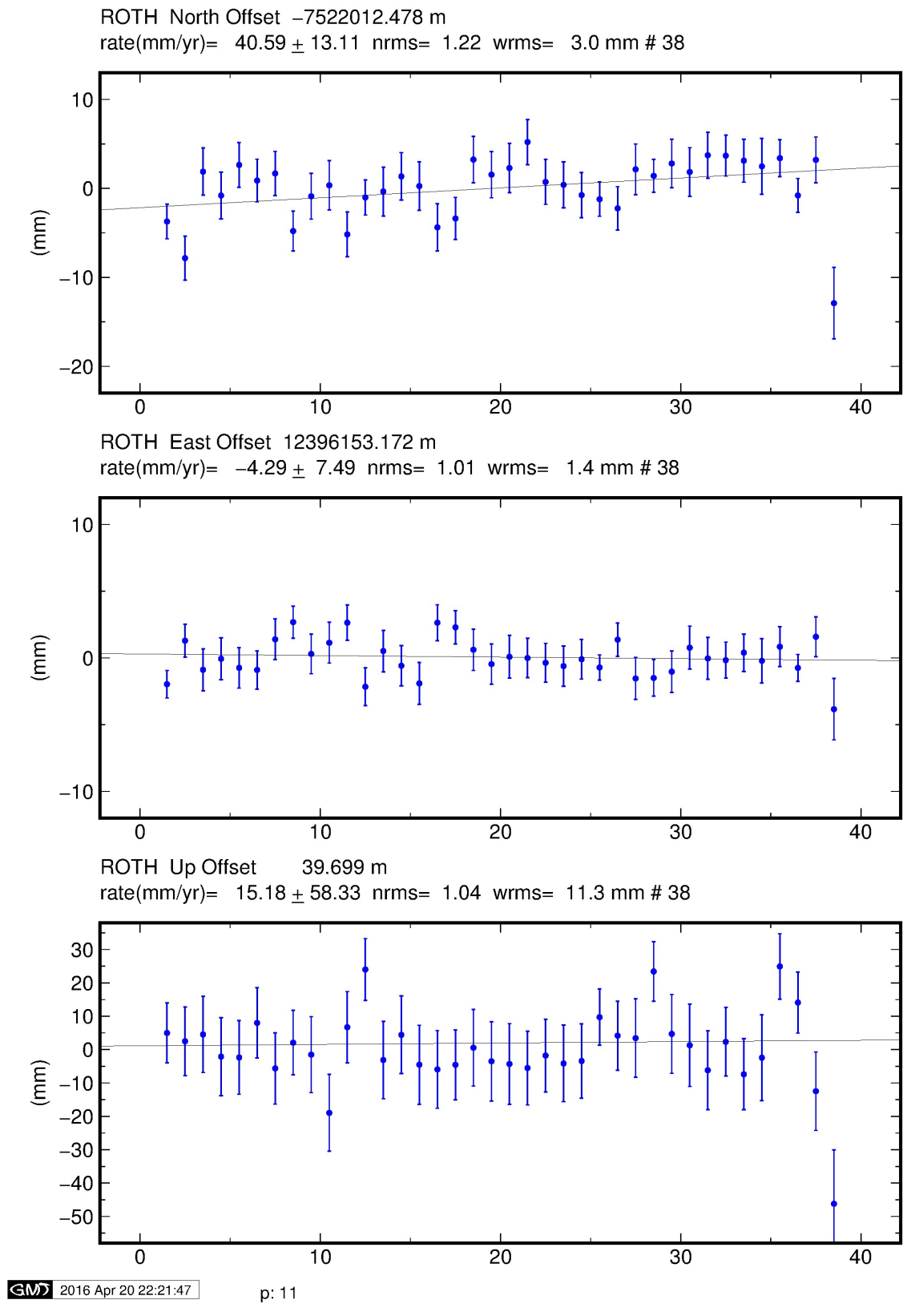

Figure 14.6: Time series for ROTH, January 2016

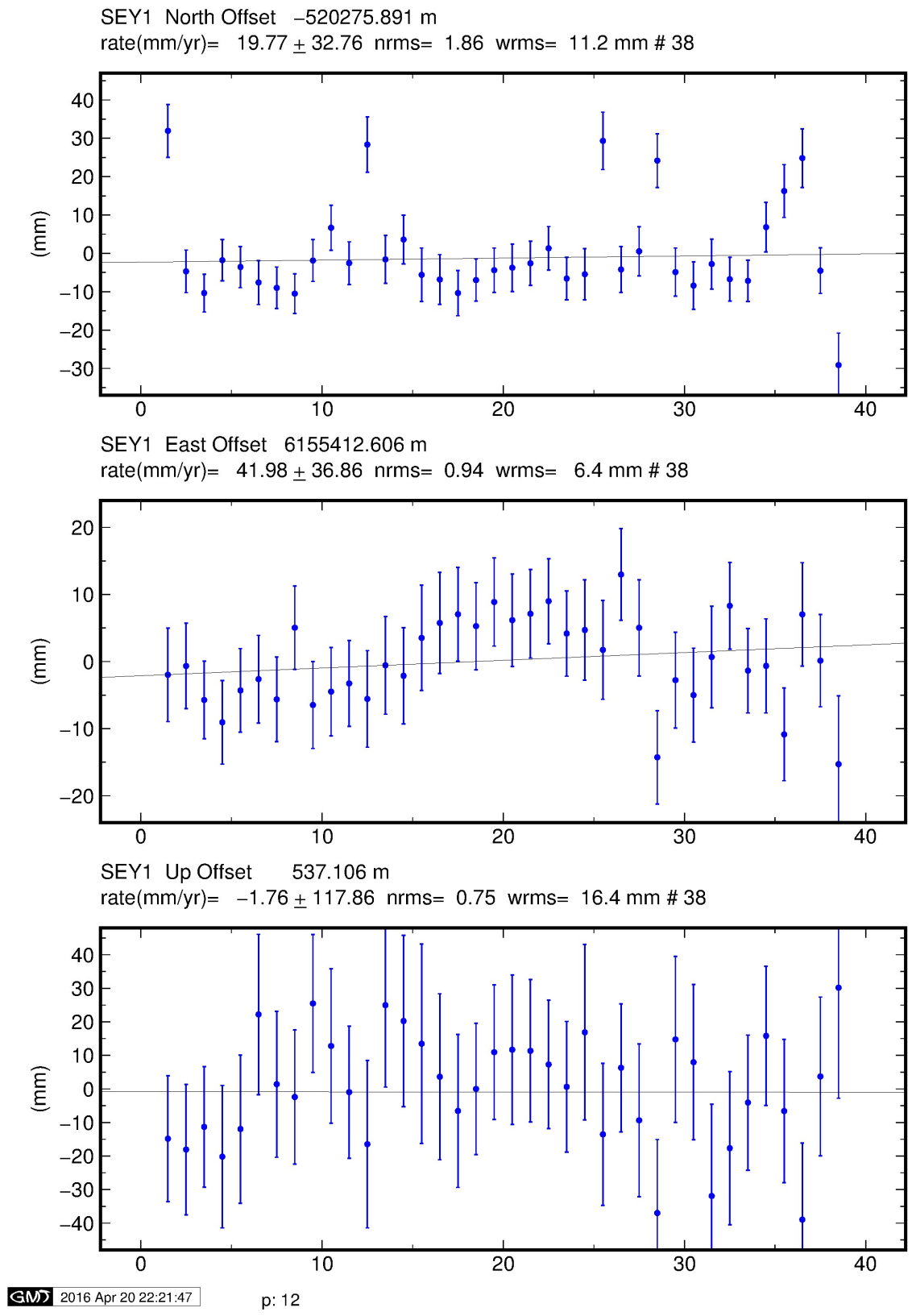

Figure 14.7: Time series for SEY1, January 2016

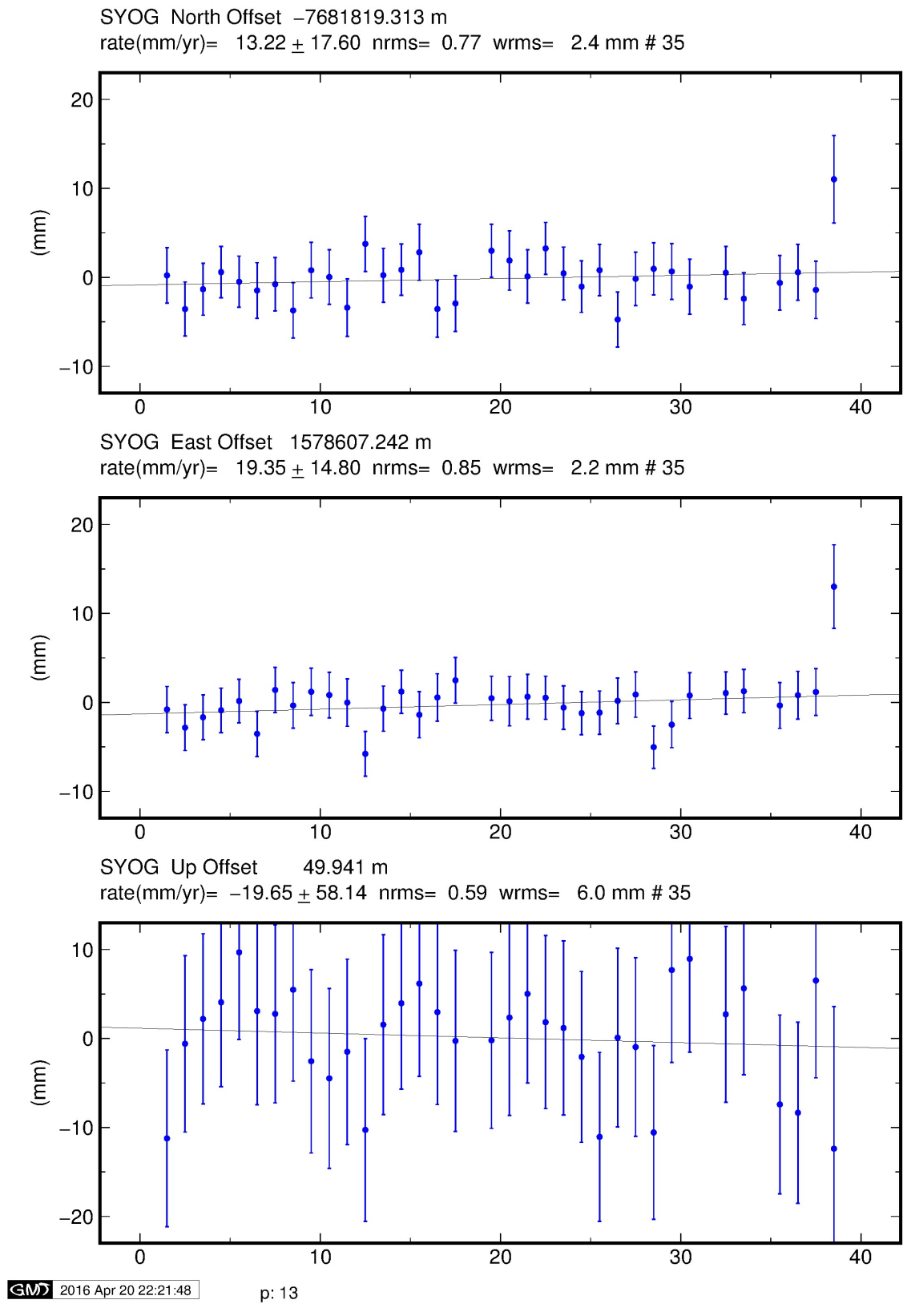

Figure 14.8: Time series for SYOG, January 2016

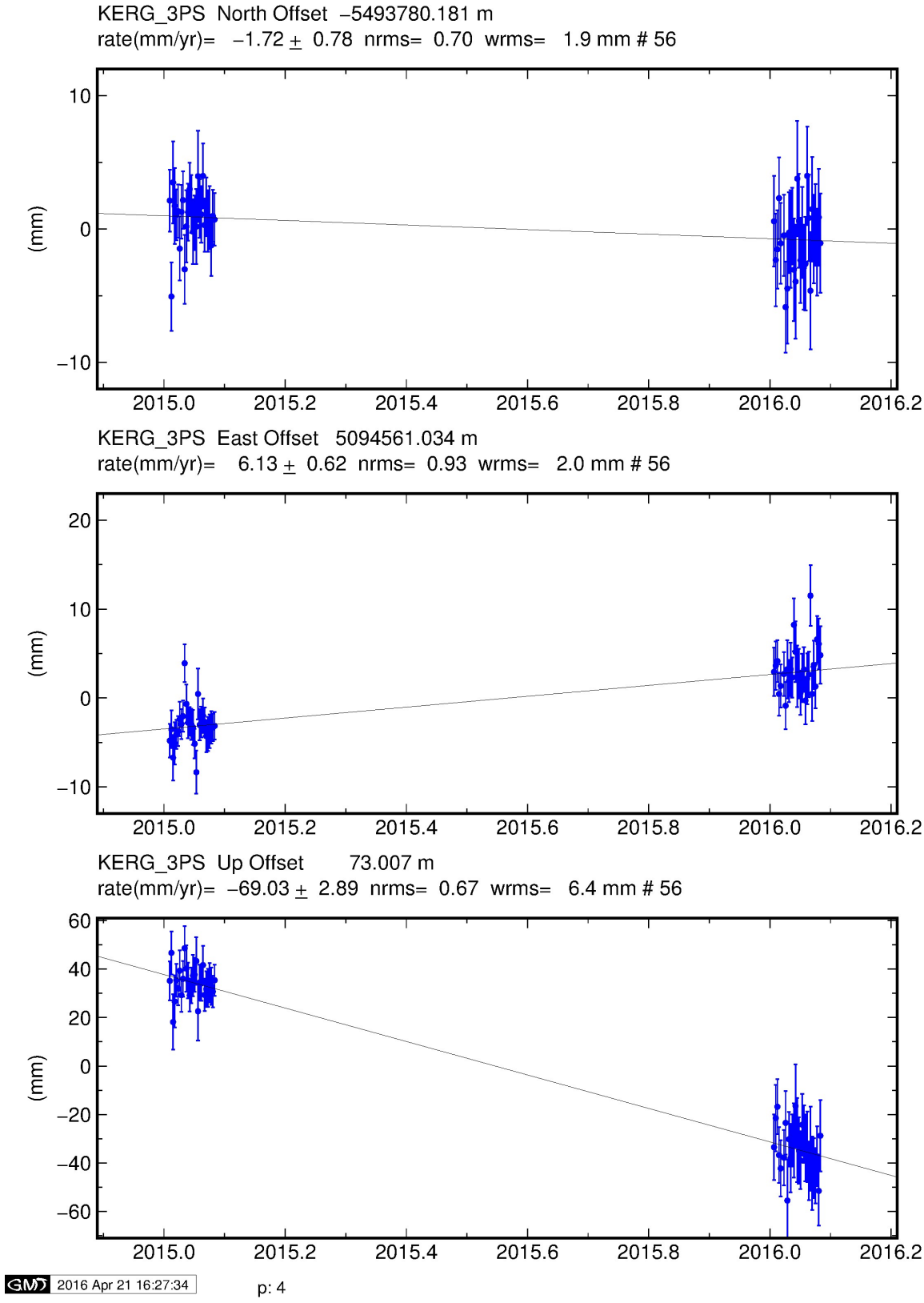

Figure 14.9: Time series for KERG, Jan 2015, and Jan 2016, showing the movement of site

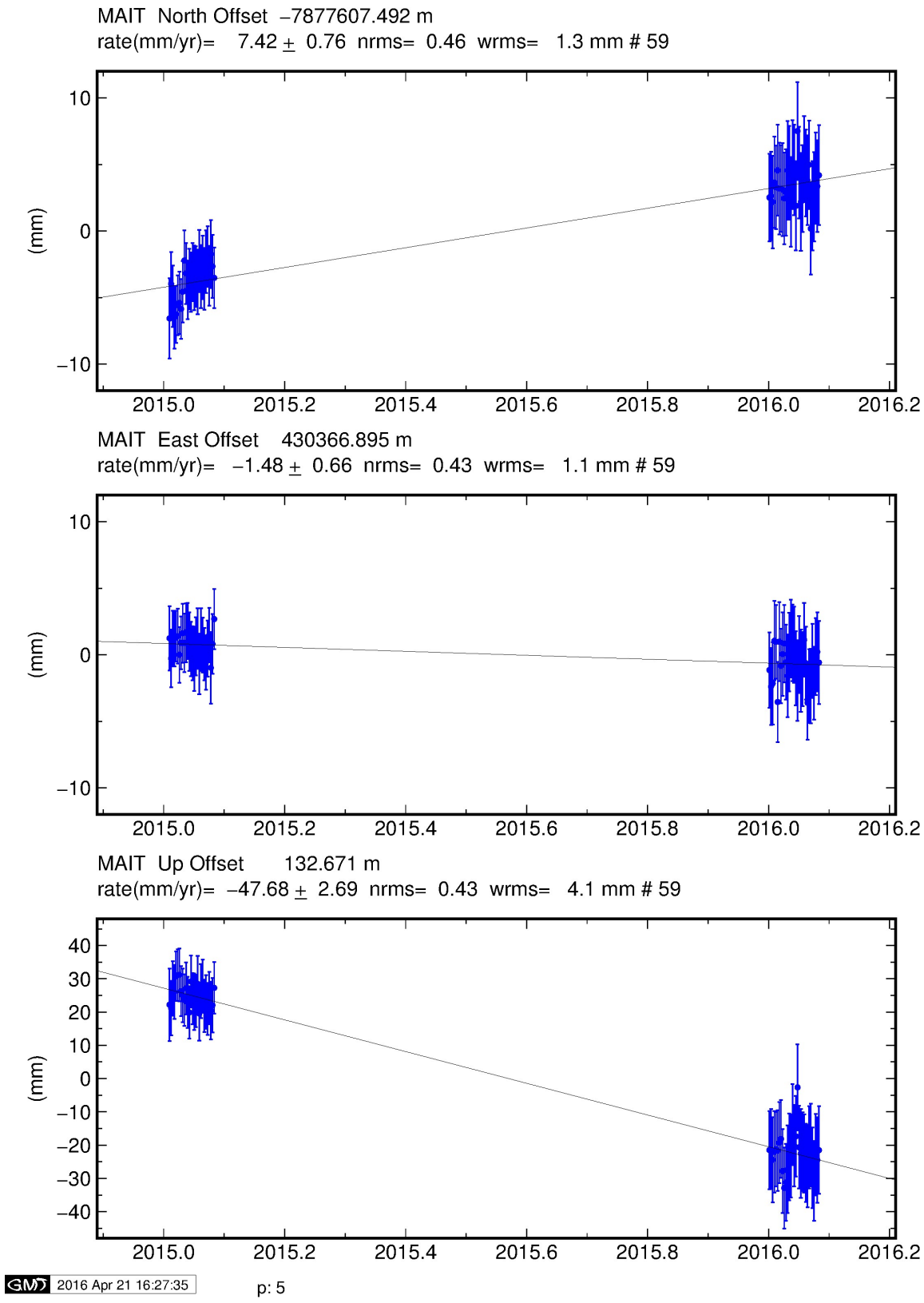

Figure 14.10: Time series for MAIT, Jan 2015, and Jan 2016, showing the movement of site

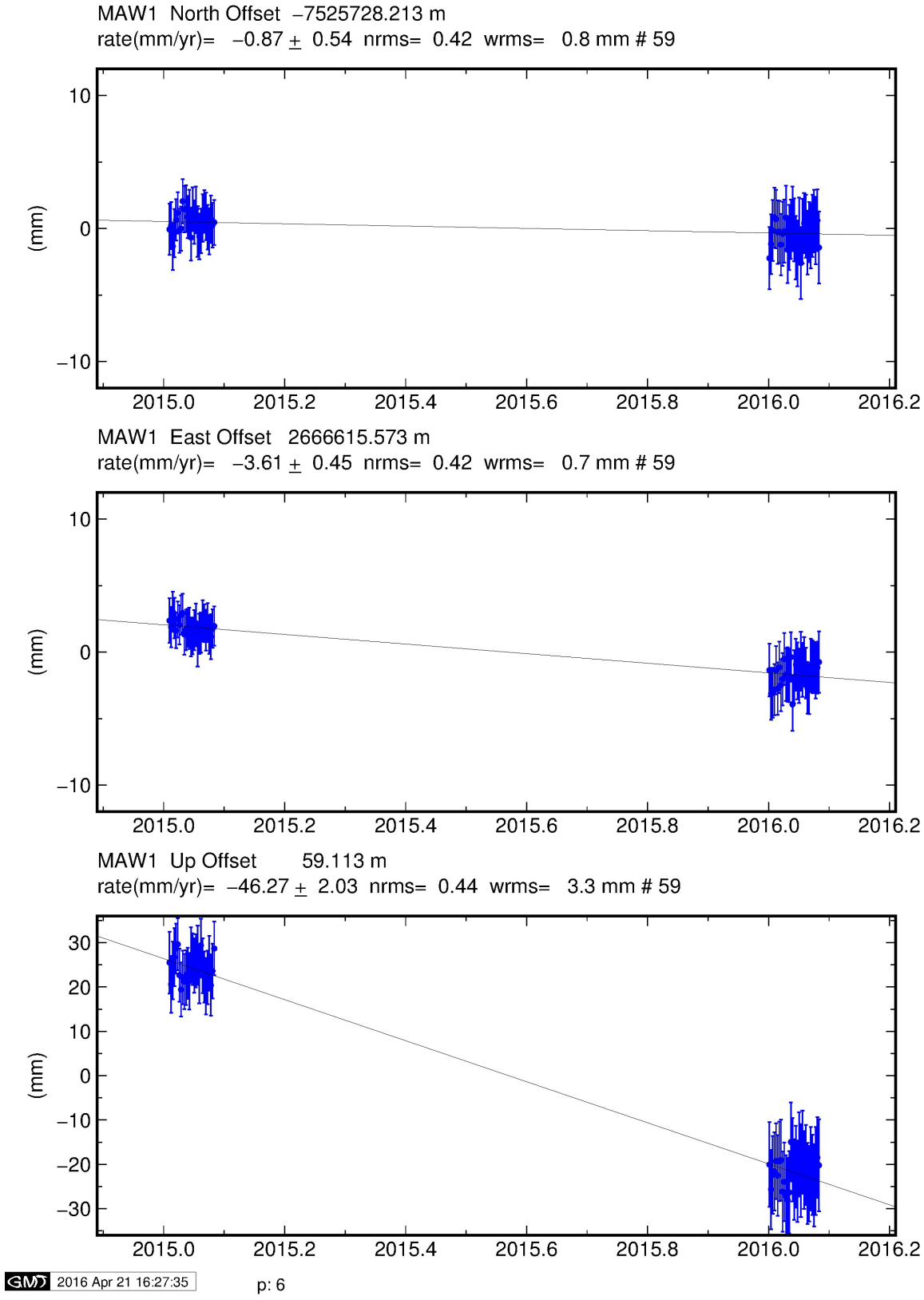

Figure 14.11: Time series for MAW1, Jan 2015, and Jan 2016, showing the movement of site

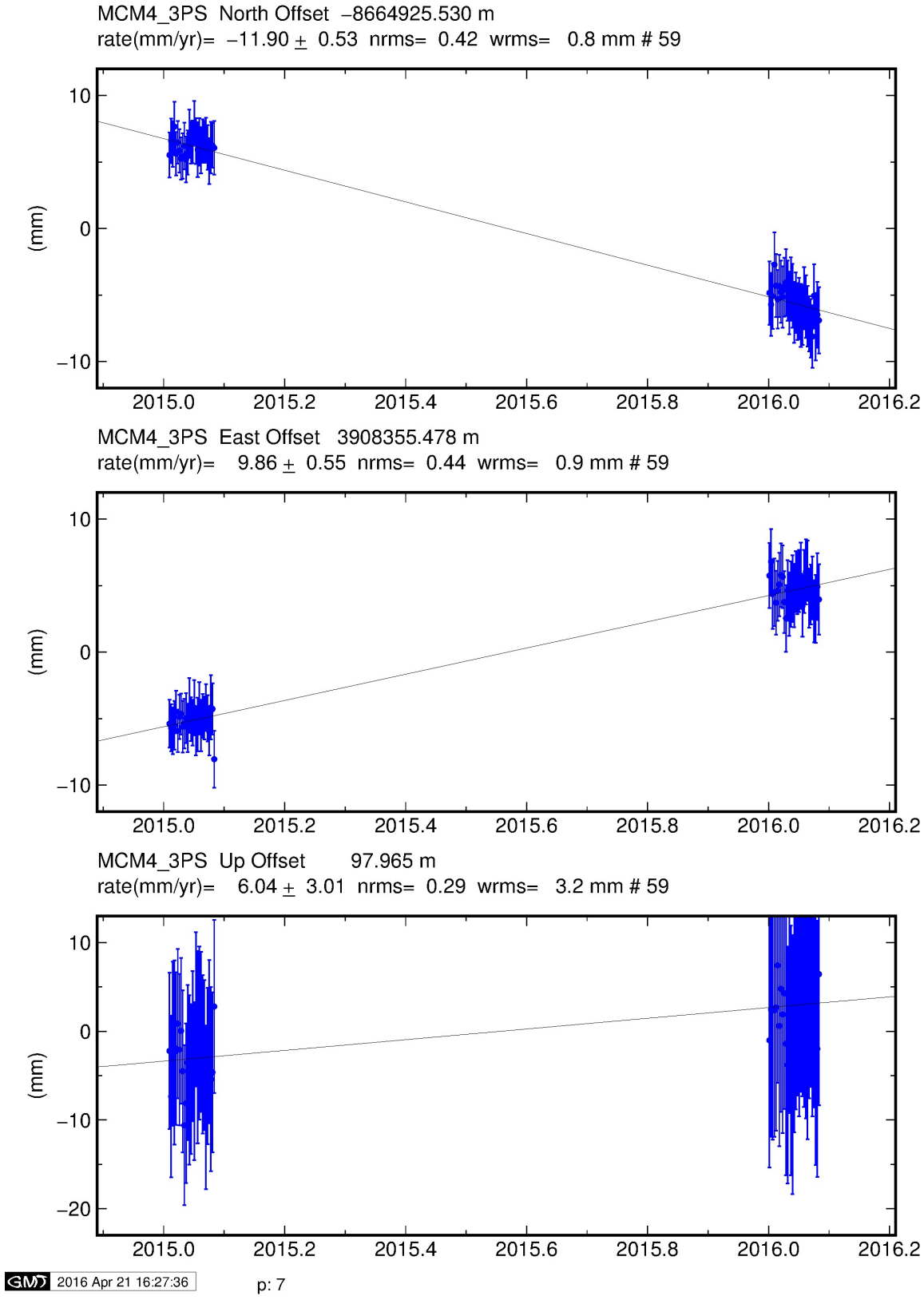

Figure 14.12: Time series for mcm4, Jan 2015, and Jan 2016, showing the movement of site

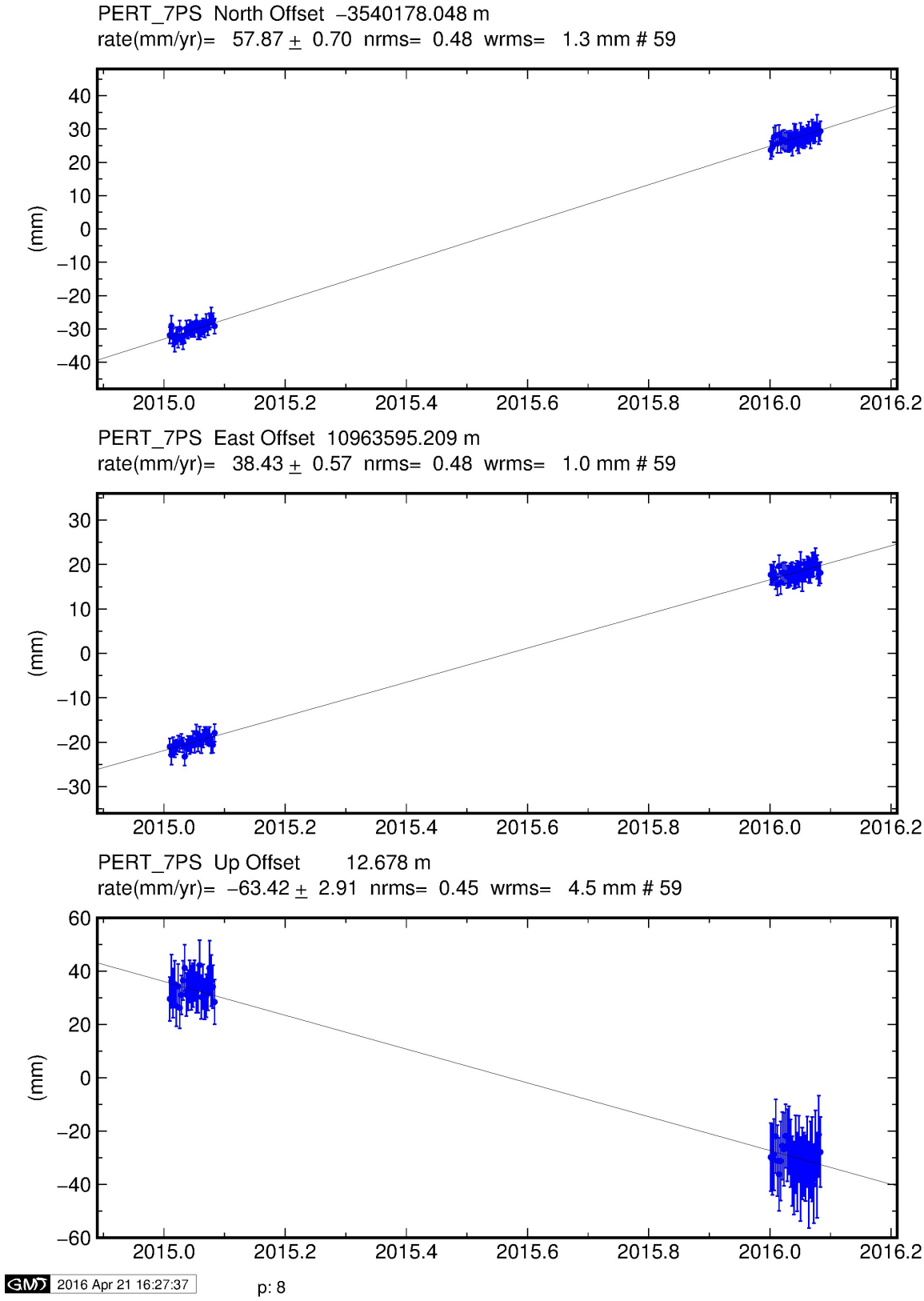

Figure 14.13: Time series for PERT, Jan 2015, and Jan 2016, showing the movement of site

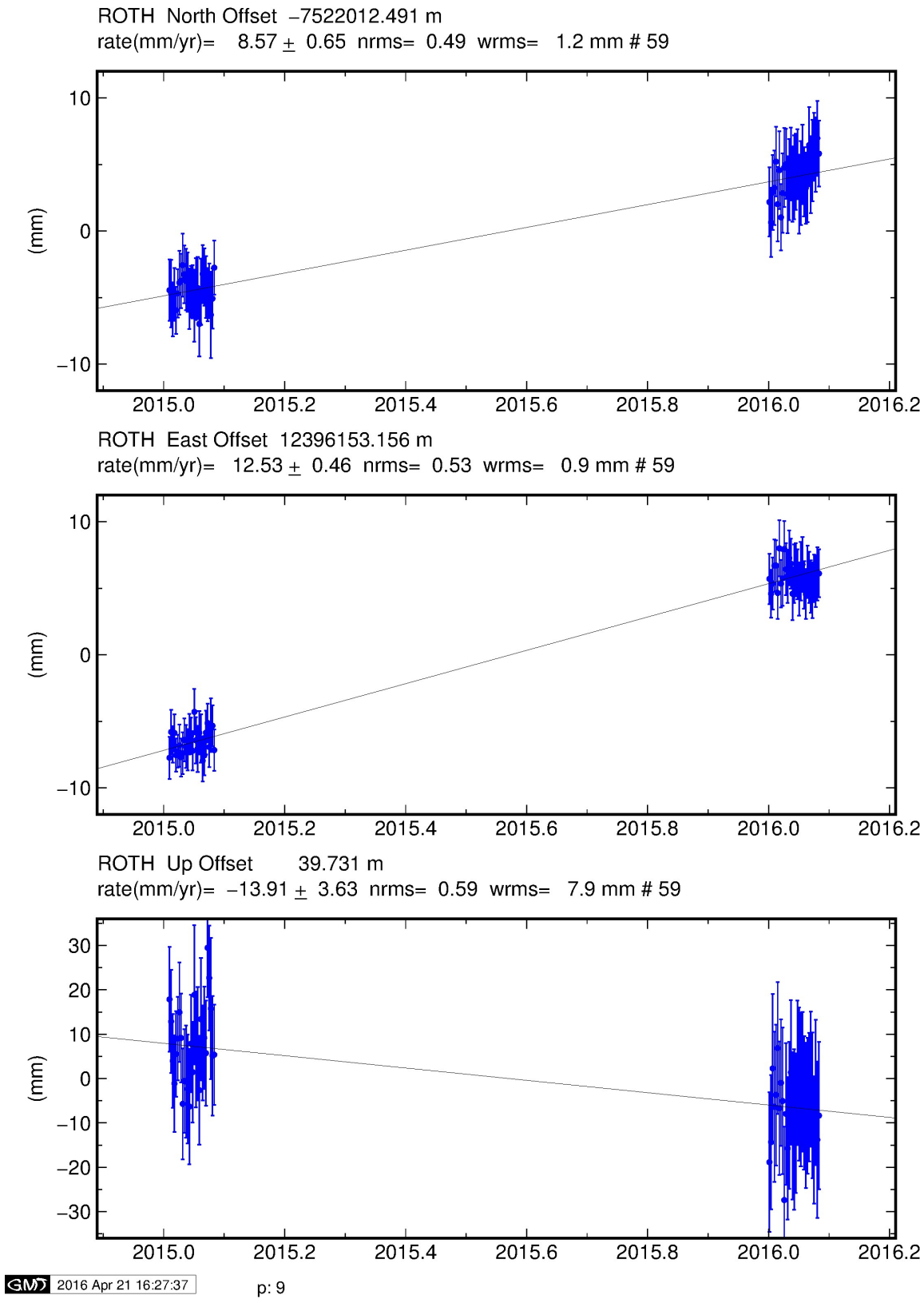

Figure 14.14: Time series for ROTH, Jan 2015, and Jan 2016, showing the movement of site

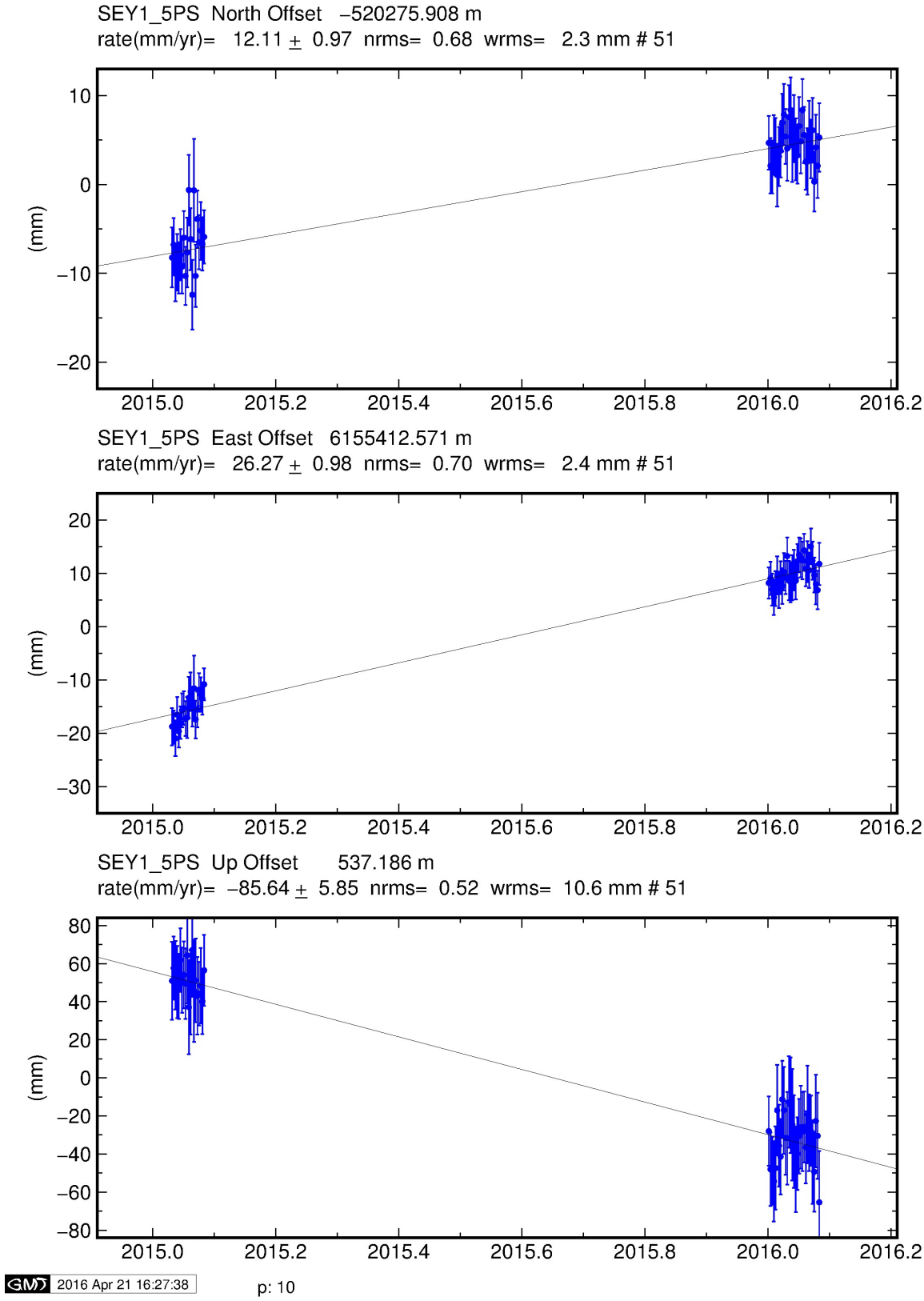

Figure 14.15: Time series for SEY1, Jan 2015, and Jan 2016, showing the movement of site

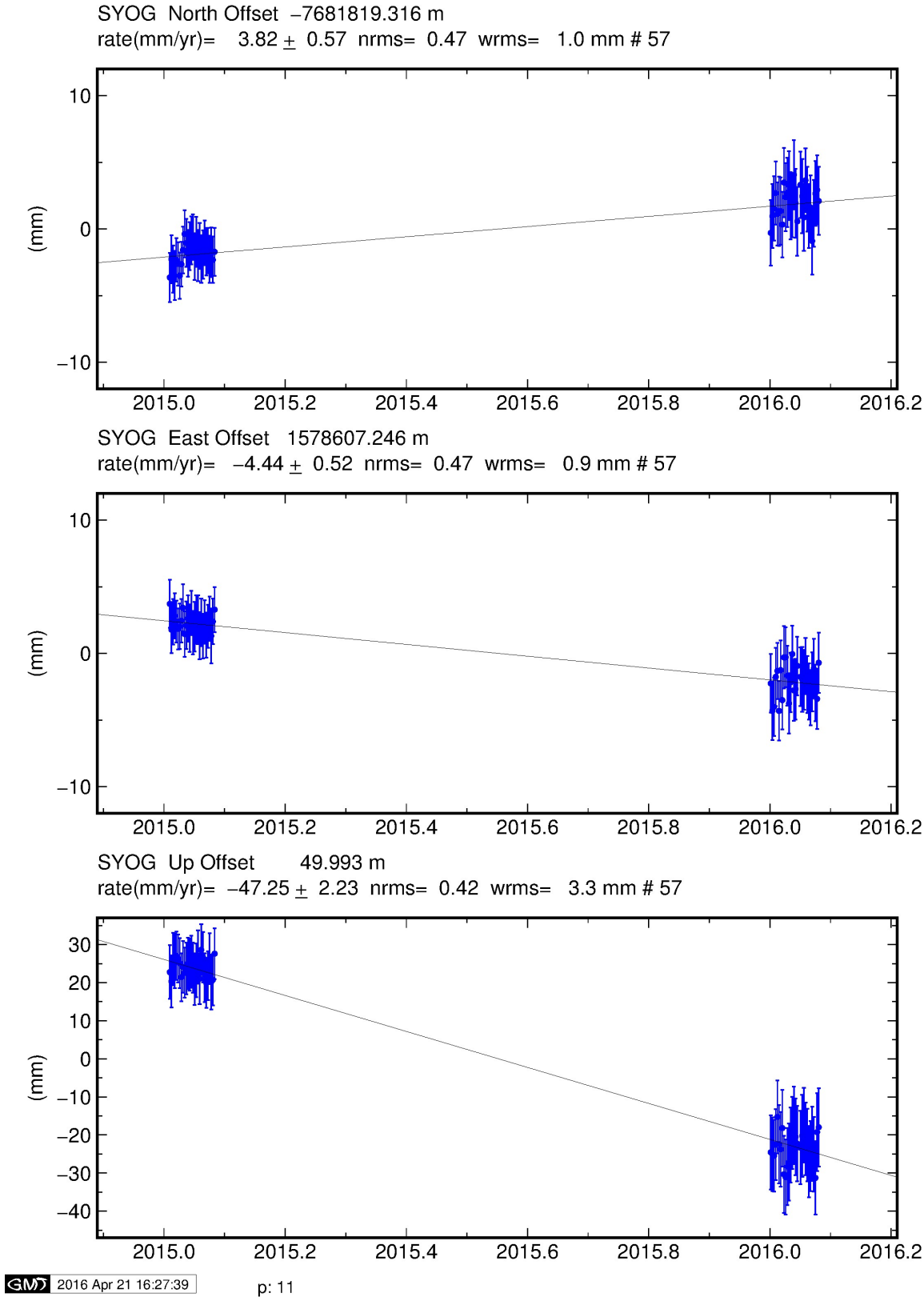

Figure 14.16: Time series for SYOG, Jan 2015, and Jan 2016, showing the movement of site

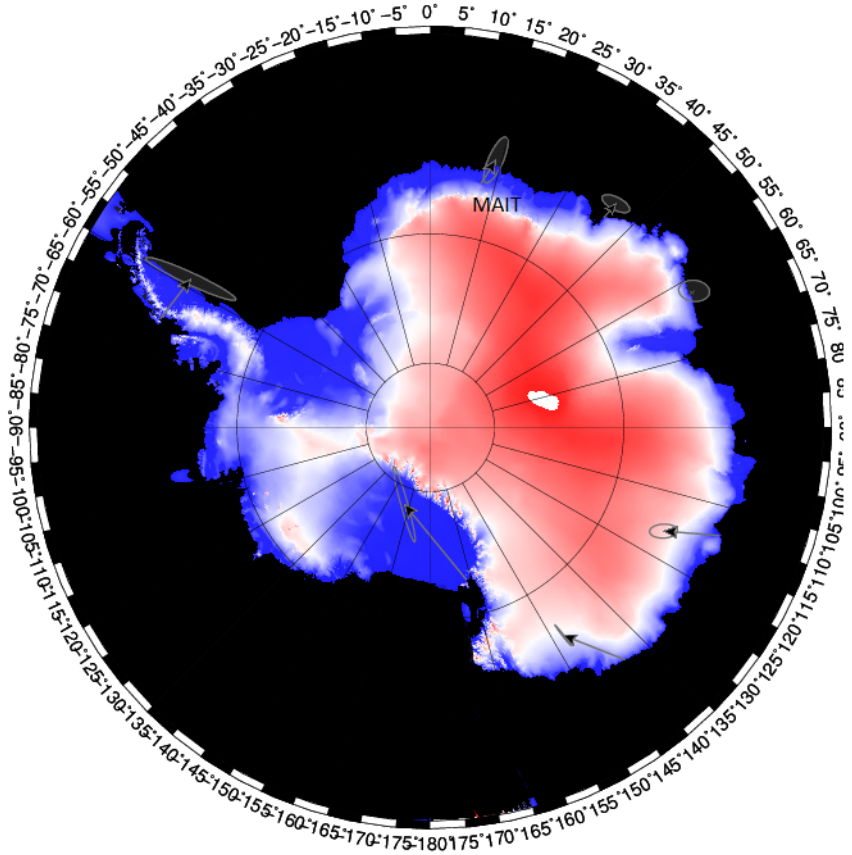

Figure 14.17: Map of Antarctica with velocity estimates

15. REFERENCES

1. Adams, R. D., Akoto, A. M. (1986). Earthquakes in continental Antarctica. Journal of geodynamics, 6(1), 263-270.

2. Argus, D. F., Peltier, W. R., Drummond, R., Moore, A. W. (2014). The Antarctica component of postglacial rebound model $ICE{-}6G_C(VM5a)$ based on GPS positioning, exposure age dating of ice thicknesses, and relative sea level histories. Geophysical Journal International, 198(1), 537-563.

3. Backus G E and Gilbert J F 1967 Numerical applications of a formalism for geophysical inverse problems Geophys. J. R. Aslron. Soc. 13, 247-76

4. Bevis, M., Kendrick, E., Smalley, R., Dalziel, I., Caccamise, D., Sasgen, I., Konfal, S. (2009). Geodetic measurements of vertical crustal velocity in West Antarctica and the implications for ice mass balance. Geochemistry, Geophysics, Geosystems, 10(10).

5. Berdichevsky, M. N., and Zhdanov, M. S., 1984. Advanced theory of deep geomagnetic sounding. Elsevier, Amsterdam, pp. 408.

6. Bouin, M. N., Vigny, C. (2000). New constraints on Antarctic plate motion and deformation from GPS data. Journal of Geophysical Research: Solid Earth (1978–2012), 105(B12), 28279-28293.

7. Cagniard, L., 1953. Basic theory of the magnetotelluric method of geophysical prospecting. Geophys., 18, 605-635

8. Cande, S. C., Stock, J. M., Müller, R. D., Ishihara, T. (2000). Cenozoic motion between east and west Antarctica. Nature, 404(6774), 145-150.

9. Cooper, A. P. R., Smellie, J. L., Maylin, J. (1998). Evidence for shallowing and uplift from bathymetric records of Deception Island, Antarctica. Antarctic science, 10(04), 455-461.

10. Dietrich, R., A. Rülke, J. Ihde, K. Lindner, H. Millerd, W. Niemeiere, H.-W. Schenkef and G. Seeber (2004). "Plate kinematics and deformation status of the Antarctic Peninsula based on GPS." Global and Planetary Change 42: 313-321. doi:10.1016/j.gloplacha.2003.12.003.

11. Dong, D., Fang, P., Bock, Y., Cheng, M. K., & Miyazaki, S. (2002). Anatomy of apparent seasonal variations from GPSderived site position time series. Journal of Geophysical Research: Solid Earth (1978–2012), 107(B4), $ETG - 9$.

12. Donnellan, A., Luyendyk, B. P. (2004). GPS evidence for a coherent Antarctic plate and for postglacial rebound in Marie Byrd Land.Global and Planetary Change,42(1), 305-311.

13. Grant, F. S., and West, G. F., 1965. Interpretation theory in applied geophysics. McGraw- HiliBook Company, New York, pp, 584.

14. Herring, T. A., Introduction to GAMIT/GLOBK

15. Kanao, M. (2014). Seismicity in the Antarctic Continent and Surrounding Ocean. Open Journal of Earthquake Research, 2014.

16. Kaufman, A.A, and Keller, G. V., 1981.The magnetotelluric sounding method. Elsevier, Amsterdam.

17. Lawver, L. A., Müller, R. D. (1994). Iceland hotspot track. Geology, 22(4), 311-314.

18. Li, Zhilin, An Overview of the Immersed Interface Method and Its Applications, Taiwanese Journal Of Mathematics, Vol. 7, No. 1, pp. 1-49, March 2003

19. Lythe, M. B., Vaughan, D. G. (2001). BEDMAP: A new ice thickness and subglacial topographic model of Antarctica. Journal of Geophysical Research: Solid Earth (1978–2012), 106(B6), 11335-11351.

20. Mitra, R., 1973. Computer techniques for electromagnetics.Pergamon, New York.

21. Morgan, M. A., (Ed.), 1990. Finite element and finite difference methods in electromagnetic scattering. Elsevier, New York.

22. Nakada, M., & Lambeck, K. (1988). The melting history of the late Pleistocene Antarctic ice sheet. Nature, 333(6168), 36-40. Parker, R.L., 1983. The magnetotelluric inverse problem. Geophys. Surv., 6: 5-25

23. Robinson, E. S., Splettstoesser, J. F. (1984). Structure of the Transantarctic Mountains determined from geophysical surveys (pp. 119-162). American Geophysical Union.

24. Singh, Arun, Development of Block Inversion Algorithm and Its Comparison with Cell Inversion Scheme(2014), M.Tech Dissertation, IIT Roorkee

25. Stern, T. A., & ten Brink, U. S. (1989). Flexural uplift of the Transantarctic Mountains. Journal of Geophysical Research: Solid Earth (1978–2012), 94(B8), 10315-10330.

26. Zhdanov, M. S., 2009. Geophysical electromagnetic theory and methods. Elsevier, Amsterdam.

27. Zhou, P. B., 1993. Numerical analysis of electromagnetic fields. Springer-Verlag, pp. 406.

28. EAS-591T – Space Geodetic Measurements of Active Crustal Motions - Purdue University

16. APPENDIX

16.1. Subroutine for IIM

```
function[a1, a2, a3, a4, a5]=get_coefficients(iy, izm1, iym1, iz2, \\
.. iy3, iz3, iyp1, iz4, iy5, izp1, delk)
    diary('iim.txt');
    disp(delk);
    diary off;
    matrixA=[1, 1, 0, 0, 0, 0, 0, delk, 0, 0, 0, 0;\\
    0, 0, 1, 1, 0, 0, 0, 0, 0, 0, 0, 0; \\
    0, 0, 0, 0, 1, 1, 0, 0, 0, 0, 0, 0; \\
    0, 0, 0, 0, 0, 0, 1, 1, 0, 0, 0, 0; \\
    0, 0, 0, 0, 0, 0, 0, 0, 1, 1, 0, 0; \\
    0, 0, 0, 0, 0, 0, 0, 0, 0, 0, 1, 1];
    matrixAT=ctranspose(matrixA);
    prod=matrixAT*matrixA;
    prod=prod+0.001*eye(12);
    global mmyl mmyr mmzu mmzd
    if((iy < mmyl && iyp1 > mmyl) || (iy > mmyl && iym1 < mmyl))
        interfacey=mmyl;
        interfacez=iz3;
    else
    if( ( iy < mmyr && iyp1 > mmyl) || (iy > mmyr && iym1 < mmyr))
          interfacey=mmyl;
          interfacez=iz3;
    else
```

```
if((iz3< mmzu && izp1>mmzu) || (iz3>mmzu && izm1<mmzu ))
        interfacey=iy3;
        interfacez=mmzu;
else
    interfacey=iy3;
    interfacez=mmzd;
end
end
end
[k1,z1]=local_coord(iy,interfacey,izm1,interfacez);
[k2,z2]=local_coord(iym1,interfacey,iz2,interfacez);
[k3,z3]=local_coord(iy3,interfacey,iz3,interfacez);
[k4,z4]=local_coord(iyp1,interfacey,iz4,interfacez);
[k5,z5]=local_coord(iy5,interfacey,izp1,interfacez);
g=zeros(12,1);
b=[0;0;0;1;1;0];
prodb=matrixAT*b;
invA=inv(prod);
g=invA*prodb;
alphas=zeros(5,1);
if((iy < mmyl && iyp1 > mmyl) || ( iy < mmyr && iyp1 > mmyl))
    matg=[1,1,1,0,1;0,0,0,1,0;k1,k2,k3,0,k5;0,0,0,k4,0;
    z1,z2,z3,0,z5;0,0,0,z4,0;k1*k1/2,k2*k2/2,k3*k3/2,0,k5*k5/2;
    0,0,0,k4*k4/2,0;z1*z1/2,z2*z2/2,z3*z3/2,0,z5*z5/2;
    0,0,0,z4*z4/2,0;k1*z1,k2*z2,k3*z3,0,k5*z5;0,0,0,k4*z4,0];
    matgt=transpose(matg);
    gmod=matgt*g;
    modmatg=matgt*matg;
    modmatg=modmatg+lambda_2*eye(5);
    invmatg=inv(modmatg);
    alphas=zeros(5,1);
    alphas=invmatg*gmod;
```

```
end
if((iy > mmyl && iym1 < mmyl) || (iy > mmyr && iym1 < mmyr))
    matg=[0,1,0,0,0;1,0,1,1,1;0,k2,0,0,0;k1,0,k3,k4,k5;
    0,z2,0,0,0;z1,0,z3,z4,z5;0,k2*k2/2,0,0,0;
    k1*k1/2,0,k3*k3/2,k4*k4/2,k5*k5/2;0,z2*z2/2,0,0,0;
    z1*z1/2,0,z3*z3/2,z4*z4/2,z5*z5/2;0,k2*z2,0,0,0;
    k1*z1,0,k3*z3,k4*z4,k5*z5];
    matgt=transpose(matg);
    gmod=matgt*g;
    modmatg=matgt*matg;
    modmatg=modmatg+lambda_2*eye(5);
    invmatg=inv(modmatg);
    alphas=zeros(5,1);
    alphas=invmatg*gmod;
end
if((iz3< mmzu && izp1>mmzu) || (iz3<mmzd && izp1>mmzd))
    matg=[0,1,1,1,1;1,0,0,0,0;0,k2,k3,k4,k5;k1,0,0,0,0;
    0,z2,z3,z4,z5;z1,0,0,0,0;0,k2*k2/2,k3*k3/2,k4*k4/2,k5*k5/2;
    k1*k1/2,0,0,0,0;0,z2*z2/2,z3*z3/2,z4*z4/2,z5*z5/2;
    z1*z1/2,0,0,0,0;0,k2*z2/2,k3*z3,k4*z4,k5*k5/2;k1*z1,0,0,0,0];
    matgt=transpose(matg);
    gmod=matgt*g;
    modmatg=matgt*matg;
    modmatg=modmatg+lambda_2*eye(5);
    invmatg=inv(modmatg);
    alphas=zeros(5,1);
    alphas=invmatg*gmod;
else
    matg=[0,0,0,0,1;1,1,1,1,0;0,0,0,0,k5;
    k1,k2,k3,k4,0;0,0,0,0,z5;z1,z2,z3,z4,0;
    0,0,0,0,k5*k5/2;k1*k1/2,k2*k2/2,k3*k3/2,k4*k4/2,0;
    0,0,0,0,z5*z5/2;z1*z1/2,z2*z2/2,z3*z3/2,z4*z4/2,0;
```

```
        0,0,0,0,k5*z5;k1*z1,k2*z2,k3*z3,k4*z4,0];
        matgt=transpose(matg);
        gmod=matgt*g;
        modmatg=matgt*matg;
        modmatg=modmatg+lambda_2*eye(5);
        invmatg=inv(modmatg);
        alphas=zeros(5,1);
        alphas=invmatg*gmod;
    end
    a1=alphas(1);
    a2=alphas(2);
    a3=alphas(3);
    a4=alphas(4);
    a5=alphas(5);
    return;
end
```